Human Molecular Genetics, 2016, Vol. 25, No. 8 1600–1618

doi: 10.1093/hmg/ddw036
Advance Access Publication Date: 11 February 2016
Original Article

ORIGINAL ARTICLE

Interactome network analysis identifies multiple caspase-6 interactors involved in the pathogenesis of HD

Sean-Patrick Riechers[1], Stefanie Butland[2], Yu Deng[2], Niels Skotte[2], Dagmar E. Ehrnhoefer[2], Jenny Russ[1], Jean Laine[3], Melissa Laroche[3,4], Mahmoud A. Pouladi[5,6], Erich E. Wanker[1], Michael R. Hayden[2,†] and Rona K. Graham[3,4,*,†]

[1]Max Delbrück Centrum für Molekulare Medizin Berlin-Buch, Berlin 13125, Germany, [2]Centre for Molecular Medicine and Therapeutics, Child and Family Research Institute, Department of Medical Genetics, University of British Columbia, Vancouver, British Columbia, Canada V5Z 4H4, [3]Department of Pharmacology and Physiology and, [4]Research Center on Aging, University of Sherbrooke, Sherbrooke, Quebec, Canada J1H 5N4, [5]Translational Laboratory in Genetic Medicine, Agency for Science, Technology and Research and [6]Department of Medicine, National University of Singapore, 117609 Singapore, Singapore

*To whom correspondence should be addressed at: Canada Research Chair in Neurodegenerative Diseases, Université de Sherbrooke, Faculté de Médecine et des Sciences de la Santé, Département de Pharmacologie et Physiologie, 3001-12ème Avenue N., Sherbrooke, Quebec, Canada J1H 5N4. Tel: +1 8193461110, ext. 70146; Fax: +1 8195645399; Email: rona.graham@usherbrooke.ca

Abstract

Caspase-6 (CASP6) has emerged as an important player in Huntington disease (HD), Alzheimer disease (AD) and cerebral ischemia, where it is activated early in the disease process. CASP6 also plays a key role in axonal degeneration, further underscoring the importance of this protease in neurodegenerative pathways. As a protein's function is modulated by its protein–protein interactions, we performed a high-throughput yeast-2-hybrid (Y2H) screen against ∼17 000 human proteins to gain further insight into the function of CASP6. We identified a high-confidence list of 87 potential CASP6 interactors. From this list, 61% are predicted to contain a CASP6 recognition site. Of nine candidate substrates assessed, six are cleaved by CASP6. Proteins that did not contain a predicted CASP6 recognition site were assessed using a LUMIER assay approach, and 51% were further validated as interactors by this method. Of note, 54% of the high-confidence interactors identified show alterations in human HD brain at the mRNA level, and there is a significant enrichment for previously validated huntingtin (HTT) interactors. One protein of interest, STK3, a pro-apoptotic kinase, was validated biochemically to be a CASP6 substrate. Furthermore, our results demonstrate that in striatal cells expressing mutant huntingtin (mHTT), an increase in full length and fragment levels of STK3 are observed. We further show that caspase-3 is not essential for the endogenous cleavage of STK3. Characterization of the interaction network provides important new information regarding key pathways of interactors of CASP6 and highlights potential novel therapeutic targets for HD, AD and cerebral ischemia.

[†]M.R.H. and R.K.G. are co-senior authors.

Received: December 3, 2015. **Revised and Accepted:** February 5, 2016

Introduction

Apoptosis, a genetically programmed form of cell death that uses caspases, is a fundamental biological process essential for development and regulating the delicate balance between life and death in cells. In neurodegenerative diseases, alterations in components of the cell death machinery occur and enhance apoptosis (reviewed in 1–3). Alterations in key components of this death cascade can also have opposite effects and cause uncontrolled cell growth or cancer (reviewed in 4,5). Caspases post-translationally modify their substrates through cleavage at specific recognition sites and cause either inactivation of the protein or a gain of function through generation of active proteolytic fragments. Activation of caspases and proteolytic cleavage of specific caspase substrates is an early, critical cellular event in several neurodegenerative diseases and ischemic brain disorders (6–23). Corroborating their role in neurodegeneration, inhibiting caspases improves neuronal health and behavioral outcomes in models of neurological disease (24–26). Furthermore, environmental enrichment strategies that delay and/or decrease cognitive deficits due to neurological abnormalities are associated with a decrease in caspase expression levels in the brain (27,28). In contrast, aging, which is characterized by a decline in learning and memory capacity, is accompanied by increased levels of some caspases (15,17,29).

Huntington disease (HD), a fatal neurodegenerative disorder characterized by progressive deterioration of cognitive and motor functions, is caused by an expansion of a trinucleotide (CAG) repeat encoding glutamine in the N-terminus of huntingtin (HTT) (30). Neurodegeneration in HD occurs initially and most severely in the medium spiny neurons of the striatum and later in the deep layers of the cortex (31). In addition to caspase activation, a long-standing hypothesis in neurological disorders such as HD and Alzheimer disease (AD) also proposes excitotoxic stress as a key mechanism underlying the pathogenesis of these diseases (6,8,10,32–41). Importantly, HD and AD share a striking number of other similarities including psychiatric symptoms and cognitive dysfunction, increased age-associated risk, neurotrophin depletion and abnormal protein folding (42). Recently, links between excitotoxic pathways, activation of specific caspases and behavioral deficits have been identified. The evidence suggests that proteolysis of particular caspase substrates may amplify the excitotoxic response and trigger activation of neuronal cell dysfunction, behavioral abnormalities and eventual cell death (6–10,15,43). A critical role for excitotoxic stress and caspase activation has also been demonstrated in several models of ischemia (18–20,22,23). Indeed, studies of patients, experimental animals and cell culture models in AD, HD and cerebral ischemia provide strong evidence of potential universal mechanisms in the early stages of pathways leading to neuronal death (reviewed in 1,2,42).

A deeper understanding of caspase substrates and the function of the proteolytic fragments produced upon cleavage is critical for elucidating the mechanism(s) underlying activation of specific apoptotic pathways. Numerous caspase substrates, and the fragments generated after cleavage, have active roles in apoptosis. Indeed, in several experimental paradigms, stress-induced generation of caspase-cleaved proteolytic fragments has been shown to trigger toxicity and amplify the cell death response (44–52). Additional evidence supporting the role of caspase-generated fragments in the pathogenesis of neurodegenerative diseases derives from studies on the caspase-resistant form of a caspase substrate. In general, inhibiting the proteolysis of a caspase substrate has been shown to provide protection against cell dysfunction and death (6–8,14,15,43,49,51,53–64).

CASP6 was originally identified as an executioner caspase due to its role in cytoskeletal alterations and cleavage of nuclear lamins. However, CASP6 has since been shown to also function as an initiator caspase through its ability to cleave initiator and executioner caspases (65–67), and activation of CASP6 is observed with aging in the brain and prior to the clinical and pathological diagnosis of both AD and HD (15,17,68,69). Furthermore, preventing CASP6 proteolytic processing of mutant huntingtin (mHTT) or amyloid precursor protein (APP) in HD and AD, respectively, or targeted deletion of CASP6 has been beneficial under these conditions (6–13,15,43,70–72), suggesting that cleavage of other CASP6 substrates may play an important role in the neurodegeneration observed in these disorders. A role for caspase cleavage (by caspase-7) is also implicated in Spinocerebellar ataxia type 7 (73).

Despite the wealth of evidence demonstrating a central role for CASP6 in neurodegenerative diseases, there has been no systematic study using a high-throughput unbiased approach to identify the CASP6 interactome. To date, some CASP6 interactors have been identified; the vast majority are substrates by previous implication in an apoptotic/disease pathway and cleavage site assessment studies (reviewed in 1). There are thus limited details regarding how CASP6 activation leads to neuronal dysfunction and cell death in neurodegenerative diseases. Here we report the first high-throughput study to determine the interacting proteins of the pro and active forms of a caspase. Delineating the global protein–protein interaction (PPI) network of CASP6 and linking proteins with known cellular functions to CASP6 provide important information regarding a key pathway involved in the pathogenesis of neurodegenerative diseases and highlight potential novel therapeutic approaches for HD, AD and ischemia.

Results

Y2H identification of the PPI network for caspase-6

In order to identify CASP6 interactors, we performed an automated Y2H screen. Plasmids were engineered to produce fusion proteins containing the LexA DNA-binding domain and human CASP6 proform (p34) or active forms (p20 and p10) and then transformed into the MATa Y2H bait strain. Constructed bait strains were then systematically and individually mated with MATα Y2H prey strains carrying GAL4 activation domain fusion constructs of ~17 000 human sequence-validated non-redundant cDNAs from the human ORFeome collection (74,75). Both the proform and the active forms of the CASP6 protein were screened in order to provide additional information about a potential role of the identified substrates and possible regulators of CASP6. After mating in a matrix-assisted approach, protein interactions were identified by yeast growth competence on selective SD4 plates as well as by β-galactosidase activity. Potential false-positive interactors were excluded from the results on the basis of a list of proteins that show up in high frequency in previous screens with diverse bait proteins. We also excluded interactors that frequently provided a signal with different other bait proteins included in the screening campaign the CASP6 constructs were part of. Based on that, a high-confidence list of CASP6 interactor proteins was generated, which includes 87 proteins that were positive in all three replica of the screen for growth competence under selective conditions *and* in addition were positive at least twice in the LacZ assay (Fig. 1A and B and Supplementary Material, Table S1). Of the proteins identified as CASP6 interactors, 30

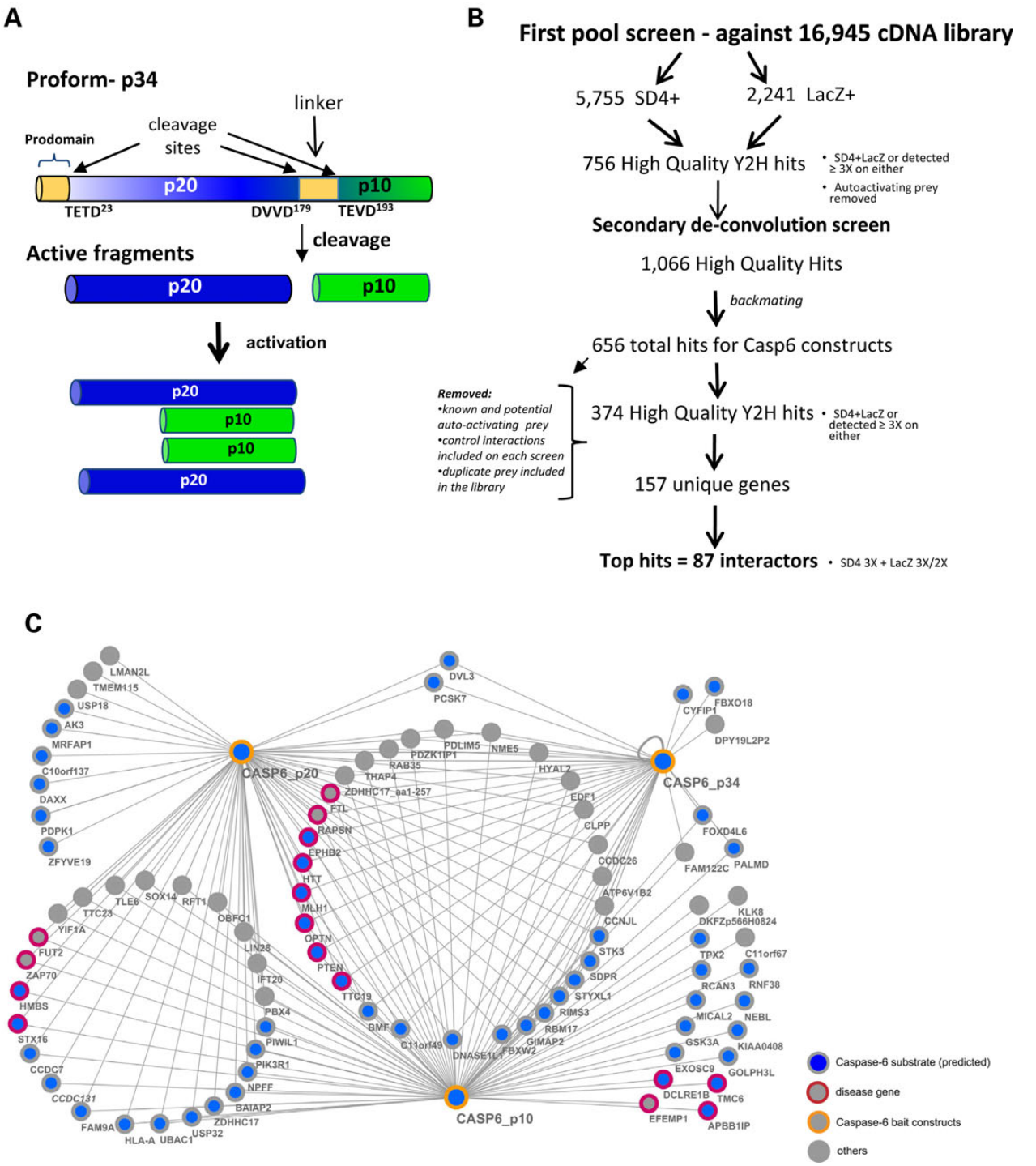

Figure 1. Results of Y2H screen with caspase-6. (**A**) Pro-CASP6 exists as a dimer with a 23aa prodomain and 14aa linker region between the large (p20) and small (p10) subunits. During activation, each CASP6 monomer is cleaved at three sites, thereby removing the prodomain and linker region. (**B**) The initial screen, including CASP6 baits p34 (proform), p20 (active form) and p10 (active form), was against a 16 945 human cDNA library. The secondary de-convolution screen included 1066 cDNAs. Top hits (87 interactors) were observed in triplicate on SD4 screen and in triplicate or duplicate on LacZ screen. (**C**) Network view of PPIs among CASP6 pro and active forms. The highest number of common interactions between CASP6 pro and active forms was observed among p34, p20 and p10 (34%). A large number of common interactions were also observed between p20 and p10 (28%).

(34%) bind to all three CASP6 baits (p34, p20 and p10). Additionally, 24 (28%) of the proteins interacted with both p20 and p10 active forms of CASP6 (Fig. 1C). Assessment of CASBAH and MEROPS databases (of caspase substrates) revealed that none of the 87 identified interactors was previously described CASP6 substrates, with the exception of HTT (6,54) and CASP6 itself [through autoactivation (76)]. We also assessed the list in Panther (77) and GO databases to determine whether there was any enrichment for specific functions and/or pathways. There was no over-representation after Bonferroni correction for function. However, there

was a significant enrichment for proteins involved in the insulin/IGF pathway-protein kinase B signaling cascade on the list of 87 interactors, compared with a genome-wide reference list ($P = 0.002$). Insulin receptors are a subgroup of receptor tyrosine kinases that are involved in modulating cell growth and metabolism.

In order to determine whether any of the CASP6 Y2H-identified interactors contain possible CASP6 recognition sites, we assessed the list through SitePrediction (78), a program that predicts the cleavage site of a protease, of which some sites are already known. SitePrediction identified 53 of 87 interactors with one or more predicted CASP6 cleavage sites with 99.9% specificity (Fig. 1C). Furthermore, 16 of 87 proteins are previously characterized disease-related proteins [OMIM database (79), Supplementary Material, Table S1].

Validation of caspase-6 Y2H interactions by LUMIER

Proteins identified in the CASP6 Y2H screen that did not contain a predicted CASP6 recognition site (28/87) were further validated using LUMIER, a luminescence-based, mammalian interaction assay (80) designed for the systematic mapping of dynamic PPI networks. Six potential casp6 substrates were also included to provide additional validation of their interaction with casp6. Assessing the PPIs identified in the Y2H study in the LUMIER assay provides additional confidence that the interaction is high quality and importantly observed in mammalian cells. All clones were tested twice in triplicate and in both possible orientations of the Renilla and Firefly tags (Renilla bait-Fire-prey/Renilla prey-Fire-bait). We accepted an interaction as positive when it was observed at least in one of the two configurations and when at least two experiments in the two repetitions were positive. The results of this experiment demonstrate that 51% of the interactions were confirmed by LUMIER (Fig. 2). A similar success rate was also observed when a positive reference set of binary interactions from the literature was examined with the LUMIER assay (81), supporting our hypothesis that high-confidence interactions were identified in our Y2H screens.

HTT interacts with caspase-6

We included several HTT fragment clones in the cDNA prey repertoire in order to determine whether an interaction between HTT and CASP6 would be detected. As expected, and detected previously (82,83), the LUMIER assay demonstrates that CASP6 interacts with fragments of wild-type (WT) and mHTT (Supplementary Material, Fig. S1). Both p34 and p20 identified the HTT clone HD507-1230 that contains the IVLD CASP6 recognition site. However, CASP6 also interacts with HTT fragments (HD513) that do not contain the 586aa putative CASP6 recognition site, suggesting that alternate binding sites for CASP6 are present in the N-terminal region of HTT, as has been suggested by previous data (82). Furthermore, in the presence of the expanded polyglutamine tract, p34 no longer interacted with the HD513 fragment. CASP6 cleavage assays confirm that CASP6 interacts with HTT and generates an ~60 kDa HTT fragment that is detected with both MAB2166 and BKP1 HTT antibodies (Fig. 3A and B), consistent with previous findings (6,54). It is important

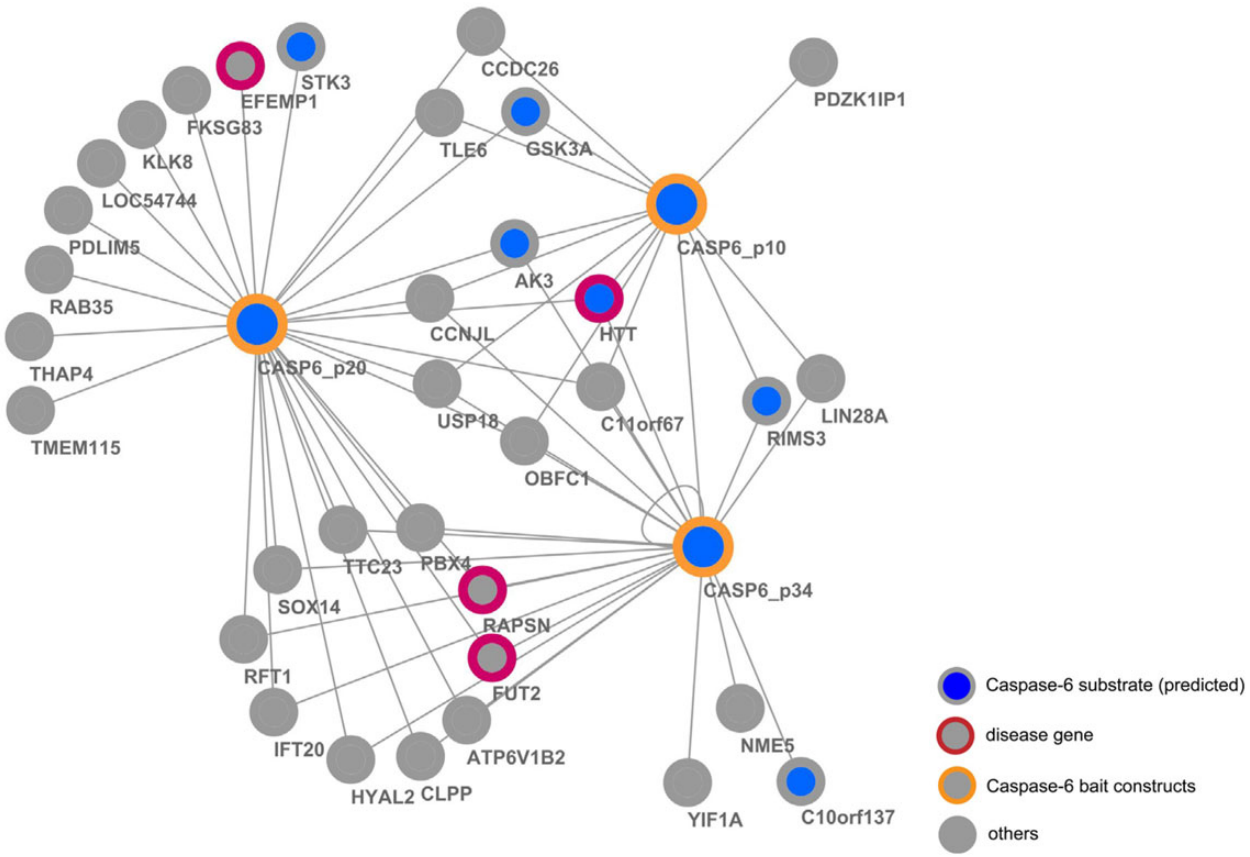

Figure 2. Confirmation of select caspase-6 Y2H-identified interactors by LUMIER. Proteins identified in the CASP6 Y2H screen that did not contain a 'predicted' CASP6 recognition site were further validated using LUMIER. Six predicted CASP6 substrates were also included to provide additional validation of an interaction with CASP6. A total of 34 proteins were screened using LUMIER and 51% of the Y2H-identified interactions confirmed.

to note that even at the lowest concentration of recombinant CASP6, the 586aa HTT fragment is detected. Indeed, in our experimental paradigm, CASP6 cleaved HTT more efficiently than all other substrates assessed. Interestingly, there was a significant enrichment of HTT interactors in the list of potential CASP6 interactors. Fully 9/87 are described HTT interactors (hypergeometric statistic = 5.6×10^{-8}, Fig. 3C).

Identification of dysregulated caspase-6 interactors in human HD brain

In order to ascertain whether the identified potential CASP6 interactors may play a role in the pathogenesis of HD, we first assessed whether expression levels of the genes identified in the screen are altered in human HD post mortem brain tissue (grades 1–4) using previously published HD mRNA profiles generated

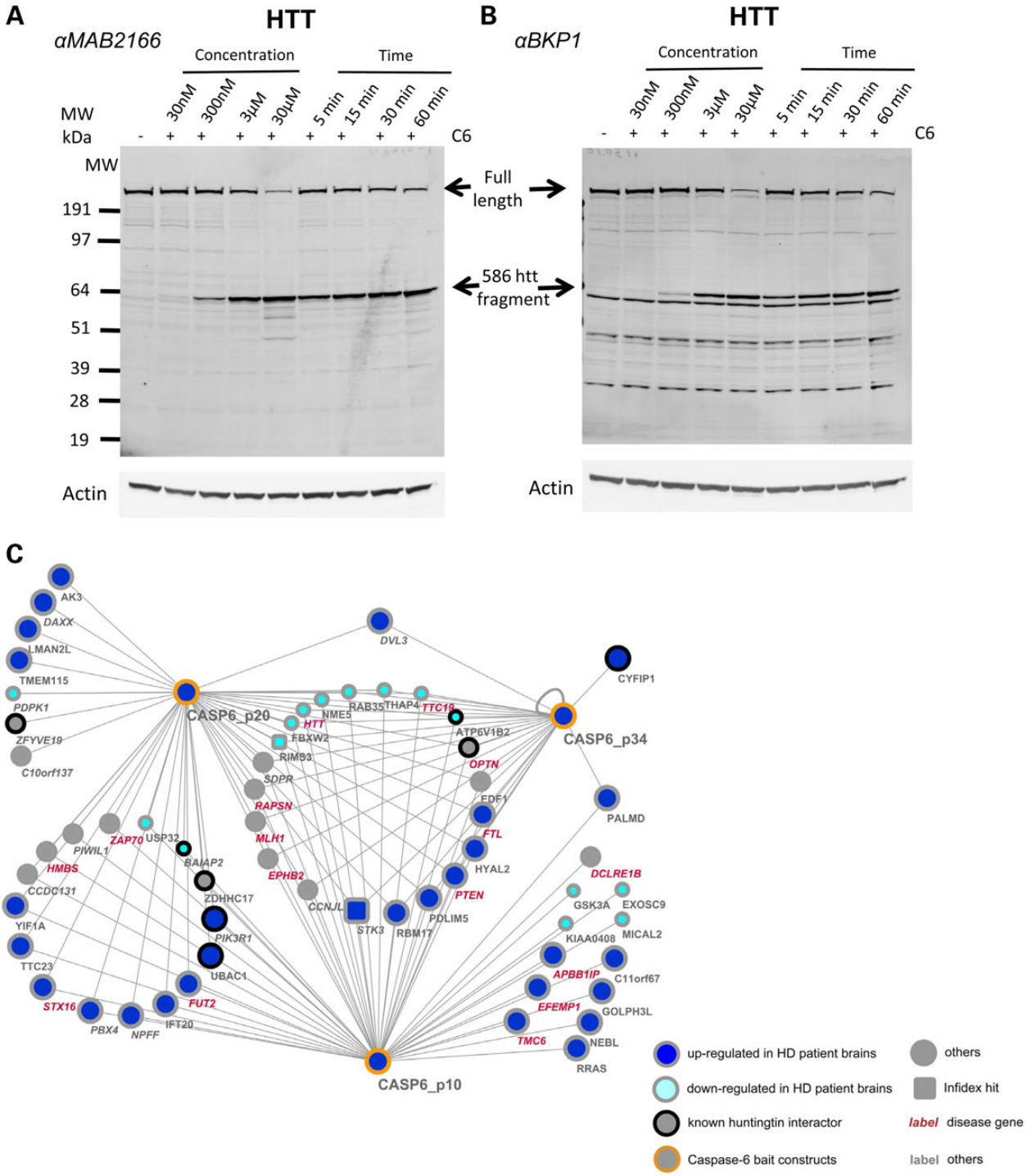

Figure 3. Several caspase-6-interacting proteins are dysregulated in HD brain. (**A**) Murine cortex lysates were subject to digestion with increasing concentrations of recombinant CASP6 for 1 h or fixed concentration of CASP6 (15 μM) and varying times of incubation. Western blotting demonstrates that CASP6 cleaves huntingtin using MAB2166 and (**B**) BKP1 HTT antibodies. (**C**) Network analysis demonstrates that a number of Y2H-identified CASP6 interactors are involved in the pathogenesis of HD. Of the 87 interactors, 47 (54%) are dysregulated in human HD brain at the mRNA level and nine are HTT interactors.

through microarray analysis (84,85). Of the 87 high-confidence interactors identified, 54% are either up- (36%) or down-regulated (18%) at the mRNA level in human HD brain when compared with control tissues (Fig. 3C and Supplementary Material, Table S2). Of note, of the genes dysregulated, 14 are altered in grade 1 post mortem HD brain. We then performed a function enrichment analysis using Panther (77) on the CASP6 interactors, showing alterations in expression levels in human HD versus control brain. A significant over-representation of the following pathways is observed: insulin/IGF pathway-protein kinase B signaling cascade ($P = 0.002$), p53 pathway feedback loops 2 ($P = 0.02$) and PI3 kinase pathway ($P = 0.02$).

We next determined whether any novel and/or previously identified CASP6 interactors showed specific alterations in the caudate nucleus (CN), the region most affected in HD using the INFIDEX method (86). By applying a three-step expression data-filtering strategy (see Materials and Methods) to all direct interaction partners of CASP6, we identified a CN-specific HD network. In the first step, 21 of 121 CASP6 interactors were shown to be differentially expressed in human brain compared with non-brain tissue, and of those, 15 were differentially expressed in the caudate. Lastly, we assessed the 15 caudate-specific CASP6 interactors to determine which were dysregulated in HD post mortem tissue compared with controls. Using this step-by-step approach, we identified a CN-specific HD network comprising six dysregulated CASP6 interaction partners, namely, STK3, VIM, TOP1, PKC, CFLAR and RIMS3 (Supplementary Material, Fig. S2).

Identification of novel caspase-6 substrates

As CASP6 is activated early in HD, cleavage of other CASP6 substrates in addition to HTT may contribute to the pathogenesis of HD. Cleavage may result in the inactivation of the protein, for example, of a pro-survival protein, and reduce the threshold for apoptosis to occur. Cleavage may also result in the generation of toxic (pro-apoptotic) fragments, which may then contribute to neuronal dysfunction and/or cell death.

From our list of 87 interactors, 24 (28%) of the proteins were identified with both the p20 and p10 active forms of CASP6. In contrast, only three (3%) proteins are in common among the p34 proform of CASP6 and p10 and two (2%) among p34 and p20 baits, supporting that some of these proteins may indeed be CASP6 substrates.

Bioinformatic approaches were used as a first step in order to prioritize the identification and characterization of possible CASP6 substrates involved in the pathogenesis of HD (Fig. 4). The program SitePrediction (78) predicts that 53/87 CASP6 Y2H-identified interactors contain at least one CASP6 cleavage site

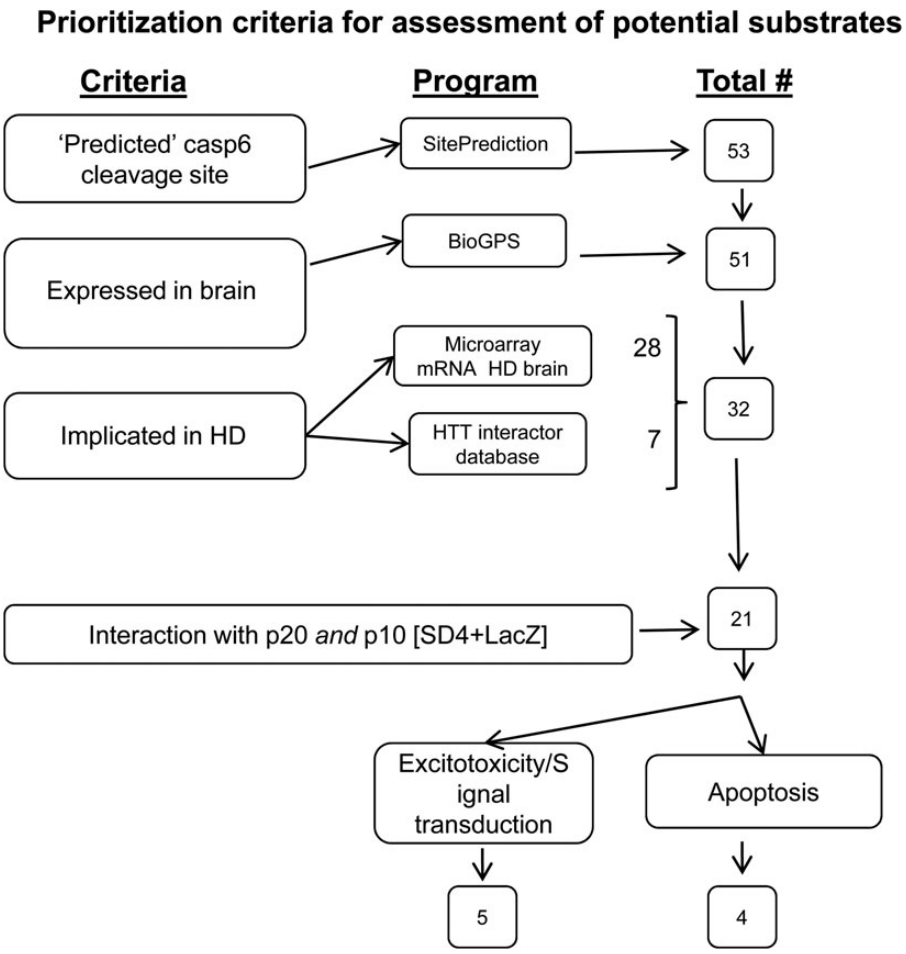

Figure 4. Criteria for selecting potential caspase-6 substrates that may play a role in the pathogenesis of HD. In order to prioritize characterization and to maximize the opportunity of identifying novel CASP6 substrates involved in the pathogenesis of HD, Y2H-identified proteins were assessed using the following criteria: (i) high likelihood of cleavage by SitePrediction (99.9% specificity), (ii) expressed in brain, (iii) implicated in HD, (iv) demonstrate an interaction with both p20 *and* p10 CASP6 baits and (v) the biological function of the protein (implicated in excitotoxicity/signal transduction and/or apoptosis pathways). The resultant proteins were then assessed in CASP6 cleavage assays.

with 99.9% specificity, 51 of which are expressed in the brain. Subsequent to this, the list was further refined by only including genes implicated in the pathogenesis of HD (alteration in expression levels in human HD brain and/or previously identified HTT interactor), which gave a list of 32 proteins.

In order to increase the likelihood of identifying substrates of CASP6, we chose only those proteins that interacted with both of the active forms of CASP6 (p20 and p10). Finally, in order to identify proteins potentially involved in key signaling pathways in HD, we determined which of the highlighted 21 proteins that bind to both active forms of CASP6 were involved in excitotoxic signaling pathways and/or apoptosis. Filtering the list in a systematic way highlighted the following nine candidates (Table 1): brain-specific angiogenesis inhibitor 1-associated protein 2 (BAIAP2), death domain-associated protein (DAXX), glycogen synthase kinase-3 alpha (GSK3A), palmdelphin (PALMD), phosphoinositide-3-kinase, regulatory subunit 1 (alpha) (P13KR1), serine threonine kinase (STK3), RNA binding motif 17 (RBM17), syntaxin 16 (STX16) and ubiquitin-specific peptidase (USP32). All candidate proteins are expressed in neurons, and due to that, a potential neuronal casp6 processing of these candidates might be disease relevant (Supplementary Material, Fig. S3). This holds true even when the candidate mRNA might be preferentially expressed in another cell type. These proteins were then assessed to determine whether they are true CASP6 substrates.

Murine cortex lysates were subject to digestion with increasing concentrations of recombinant CASP6 for 1 h or fixed concentration of CASP6 and varying times of incubation. Western blotting demonstrates that CASP6 cleaves DAXX (Fig. 5A and B), STK3 (Fig. 5C and D), USP32 (Supplementary Material, Fig. S4A and B), PALMD (Supplementary Material, Fig. S4C and D), RBM17 (Supplementary Material, Fig. S5Aand B) and STX16 (Supplementary Material, Fig. S5C and D). Diagrams of each substrate are included, which highlight structural domains and potential cleavage sites.

Major CASP6-generated fragments observed for DAXX include 20, 30 and 60 kDa C-terminal fragments. For STK3, we observed two N-terminal fragments of 35 and 45 kDa, for USP32 N-terminal fragments of 80 and 100 kDa, for PALMD 20 and 55 kDa C-terminal fragments, for RBM17 a 60 kDa fragment and for STX16 a 30 kDa fragment. All fragments detected contain the epitope for the antibody used and are of expected sizes based on SitePrediction, with the exception of RBM17 and USP32. Cleavage by CASP6 would not generate an 80 kDa USP32 fragment based on SitePrediction-predicted (99.9% specificity) cleavage sites. However, it cannot be ruled out that another protease may cleave the CASP6-generated USP32 fragment, thus resulting in a smaller-sized fragment than expected. With regard to RBM17, no predicted sized fragments were observed. However, we did detect a band at ~70 kDa in size that is cleaved by CASP6. The predicted molecular weight of RBM17 is 45 kDa. However, a form of this protein might run higher due to the acidic nature of this protein (pI 5.76) and/or numerous phosphorylation sites (87). Indeed, four separate RBM17 antibodies, which have different epitopes, detect the ~70 kDa band (see Materials and Methods).

No cleavage fragments were detected after incubation with recombinant CASP6 for BAIAP2, GSK3A or PIK3R1 (Supplementary Material, Fig. S6A and C). Overall CASP6 substrate validation of SitePrediction results had a success rate of 67%, but in each case SitePrediction did over-predict the number of CASP6 cleavage sites (Table 2). However, this does not exclude the possibility that some fragments may have high turnover rates, that the antibody did not recognize particular fragments and/or that the concentration of recombinant CASP6 in our assay was insufficient for certain proteins.

There are now 172 confirmed CASP6 interactors (Supplementary Material, Table S3). We included previously published, validated CASP6 interactors (reviewed in 1) and considered preys from the high-confidence list that interacted with at least one CASP6 bait in independent assays in both yeast and in mammalian cells as valid interactors. Performing Panther (77) analysis on this list reveals a significant over-representation of several key signaling pathways post Bonferroni correction, including FAS signaling, HD, apoptosis signaling, gonadotropin-releasing hormone receptor and AD-presenilin pathway. There is also a significant enrichment for certain molecular functions including structural constituents of the cytoskeleton, structural molecule activity, protein binding, cysteine-type peptidase activity and peptidase inhibitor activity and protein classes including cytoskeletal proteins, intermediate filament, structural proteins, actin family cytoskeletal proteins and proteolysis (Table 3).

Table 1. Top CASP6 Y2H-identified potential CASP6 substrates that may play a role in the pathogenesis of HD

Gene symbol	Dysregulated in human HD brain	Excitotoxicity/signal transduction	Apoptosis
BAIAP2	↓[a] ↓[b]	✓	
GSK3A	↓[a]	✓	
STX16	↑[a] ↑[b] ↑[c]	✓	
PALMD	↑[a]	✓	
P13KR1	↑[a] ↑[b]	✓	
DAXX	↑[a]		✓
STK3	↑[a] ↑[b]		✓
USP32	↓[a]		✓
RBM17	↑[a] ↑[b]		✓

[a]In grades 1–4 human HD brain versus control.
[b]In grade 1 human HD brain versus control.
[c]In HD astrocytes versus control.

Alterations in STK3 observed in cellular model HD

We next evaluated whether full length (FL) and/or fragment levels of the pro-apoptotic kinase STK3 demonstrate alterations in an acute model of HD. STK3 is a stress-activated pro-apoptotic kinase that upon activation and cleavage enters the nucleus and induces cell death pathways (88–90). We chose to focus on STK3 as alterations in its expression are observed in early grade human HD caudate (84,85), caspase cleavage is required for activation and toxic fragments are translocated to the nucleus (90) (a key site of pathology in HD) and the fact that STK3 negatively regulates AKT (91), a key protein involved in the pathogenesis of HD (reviewed in 92). Immortalized murine striatal cells with ($STHdh^{Q111}$) and without ($STHdh^{Q7}$) mHTT were serum-starved and assessed for protein expression of STK3 using western blotting (Fig. 6A). Activation of CASP6 is observed in this HD model (N. Skotte, personal communication) and is associated with increased cell death (93). A significant increase in FL levels of STK3 is observed in striatal cells expressing mHTT compared with WT at baseline [Fig. 6B, analysis of variance (ANOVA) $P = 0.017$, *post hoc* $P < 0.05$]. Importantly, a significant increase in the 35 kDa STK3 fragment levels is observed in neurons expressing mHTT when compared with WT cells after serum starvation (Fig. 6C, ANOVA $P \leq 0.0001$, *post hoc* $P < 0.0001$). Evaluation of lactate dehydrogenase (LDH) release (marker of cell death) demonstrates that cell death is observed with serum starvation in this model, consistent with previous findings (93) (Fig. 6D,

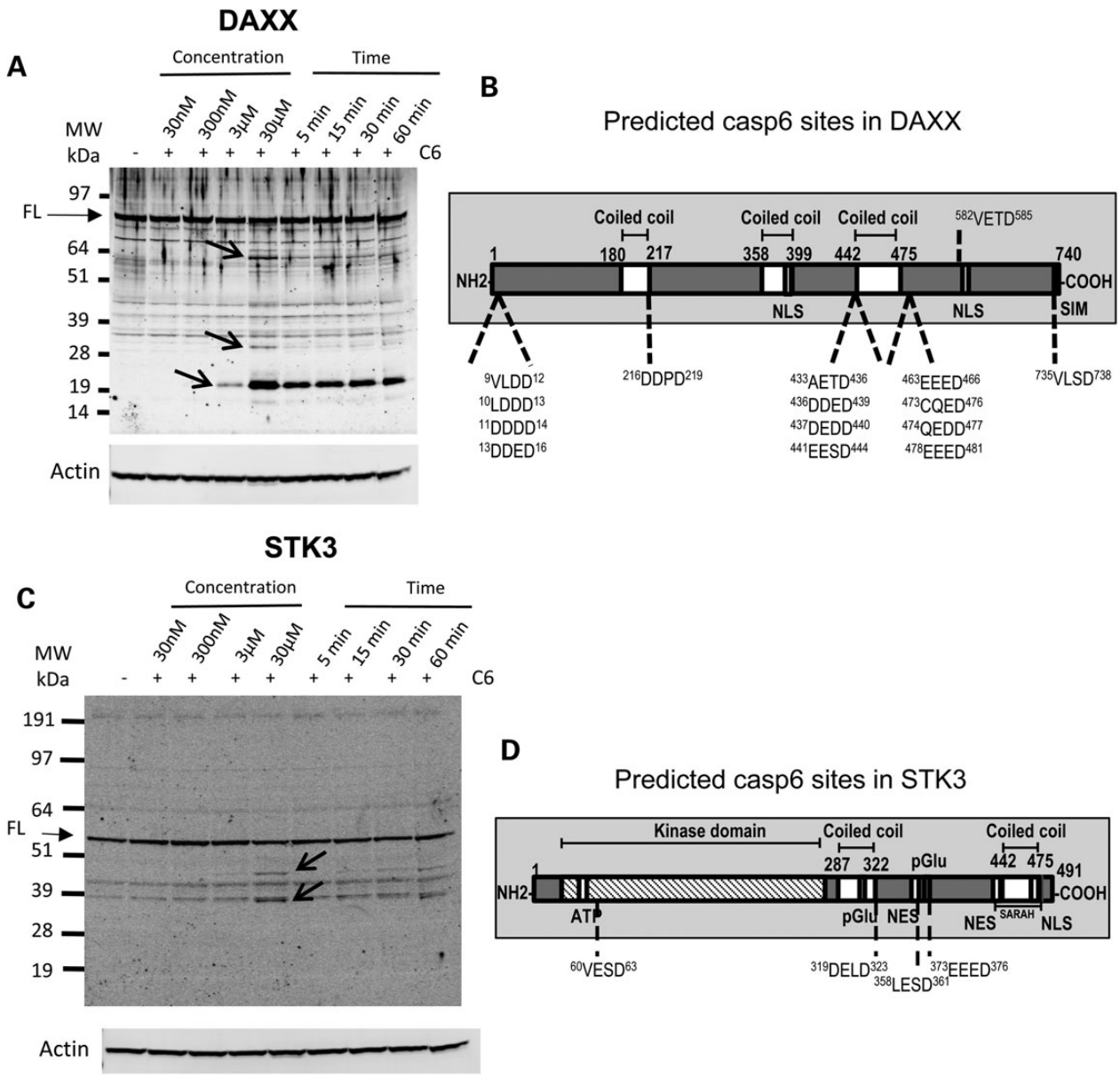

Figure 5. Novel CASP6 substrates STK3 and DAXX identified. Murine cortex lysates were subject to digestion with increasing concentrations of recombinant CASP6 for 1 h or fixed concentration of CASP6 (15 μM) and varying times of incubation. Western blotting demonstrates that CASP6 cleaves (**A**) death domain-associated protein (DAXX). (**B**) Diagram of DAXX protein showing structural (coiled coil) and NLS motifs. CASP6 also cleaves (**C**) serine–threonine kinase (STK3). (**D**) Diagram of STK3 protein showing structural (coiled coil), kinase domain and adenosine 5′-triphosphate (ATP) motifs. Major cleavage fragments are highlighted by arrows. FL, full-length form of protein. Predicted CASP6 recognition sites are shown.

3 h −serum versus +serum, $P > 0.05$; 12 h post starvation, Q111, $P < 0.01$).

Cleavage of STK3 in the absence of caspase-3

As caspase cleavage of STK3 has only been previously attributed to caspase-3 (CASP3) in the literature (90), we next wished to determine whether cleavage of STK3 occurs in the absence of CASP3. We first show that both recombinant CASP3 and CASP6 generate the same ~35 kDa fragment, whereas cleavage with CASP6 generates additional 40 and 45 kDa fragments (Fig. 7A).

Importantly, we show that cleavage of STK3 is observed in stressed MCF7 cells, which do not contain CASP3 (94). Western blotting demonstrates that MCF7 cells stressed with camptothecin show a decrease in FL STK3 levels and increase of STK3 fragments compared with unstressed MCF7 cells (Fig. 7B). These data demonstrate that CASP6 is able to cleave STK3 and that under conditions of stress STK3 cleavage fragments are generated in the absence of CASP3.

Discussion

Substantial evidence supports a central role for CASP6 in neurodegenerative diseases (6–13,15–17,29,47,48,82,95–97). Activation of CASP6, and not other caspases, is observed before onset of motor abnormalities in human and murine HD brain, and active CASP6 levels inversely correlate with age of onset of HD (15). Human AD brain also shows a significant increase in CASP6

Table 2. Summary of CASP6 Y2H-identified interactors assessed in CASP6 cleavage assays

Gene symbol	Predicted CASP6 sites (SitePrediction)	Validated (cleavage assay)	No. of cleavage fragments
DAXX	15	YES	7
PALMD	7	YES	4
USP32	5	YES	3
PIK3R1	5	NO	0
RBM17	5	YES	1
STK3	3	YES	2
BAIAP2	2	NO	0
STX16	2	YES	1
GSK3A	1	NO	0

Table 3. Result of Panther analysis on validated CASP6 interactors

	P-value	Fold enrichment
Pathway		
FAS signalling	$P = 7.05 \times 10^{-10}$	>5
HD	$P = 1.94 \times 10^{-8}$	>5
Apoptosis signaling	$P = 3.84 \times 10^{-6}$	>5
Gonadotropin-releasing hormone receptor	$P = 0.002$	>5
AD-presenilin	$P = 0.004$	>5
Molecular function		
Structural constituents—cytoskeleton	$P = 1.93 \times 10^{-1}$	4.9
Structural molecular activity	$P = 5.98 \times 10^{-9}$	3.6
Protein binding	$P = 2.03 \times 10^{-6}$	2.3
Cysteine-type peptidase activity	$P = 0.0003$	>5
Cytoskeletal protein binding	$P = 0.004$	>5
Peptidase inhibitor activity	$P = 0.003$	>5
Protein class		
Cytoskeletal	$P = 9.36 \times 10^{-14}$	>5
Anatomical structural	$P = 1.79 \times 10^{-10}$	>5
Metabolic process	$P = 3.14 \times 10^{-7}$	1.6
Intermediate filament	$P = 5.74 \times 10^{-6}$	>5
Actin cytoskeletal	$P = 0.0005$	4.4
Proteolysis	$P = 0.0004$	3.2

All values are after Bonferroni correction.

mRNA (95) and active CASP6 (16,17,96). Furthermore, in human brain, levels of CASP6-cleaved-tau correlate with global cognitive scores, emphasizing the early nature of CASP6 activation in the degenerative process of AD (17). It is crucial to understand the CASP6 network in order to identify victims and other key players in the cell death pathway. We identified 87 potential CASP6 interactors, 54% of which show alterations in mRNA expression in human HD brain, and we validated six novel CASP6 substrates. We further show that protein expression levels and cleavage of STK3, a novel CASP6 substrate identified, are altered in striatal cells expressing mHTT.

In order to understand the dynamic nature of a protein and the pathways in which it is operative, it is important to have a more global view of its function in a biological system. Several innovative approaches, including LC-MS/MS and mRNA display, have been used to identify caspase interactors including substrates (98–100). However, this is the first time that a Y2H and LUMIER screening approach has been employed using both the proform and the active form of a caspase to identify a caspase interactome. In general, overlap between Y2H and MS-based screens is low (~2–5%), suggesting that method-specific biases exist and support studies to validate the interaction directly and/or use multiple methods as we have employed here. One explanation for the occurrence of false negatives in Y2H studies is the lack of the interaction domain in the prey as for numerous proteins only a section of the protein can be expressed. However, this is not the case for our screen. Furthermore, the high stringent nature of the Y2H assay will mean that transient interactions, and/or proteins with low expression, may escape detection (101,102). Also of consideration and a potential source of bias is that some proteins may not fold properly in yeast and may require post-translational modifications not found in yeast and/or an inability of interacting protein to enter the nucleus. It is important to note that our studies used human cDNA clones and we also performed the interaction assay in mammalian cells.

Numerous caspase substrates have active roles in apoptosis, particularly as a result of the fragments generated after cleavage. Proteolytic cleavage of specific caspase substrates is an important cellular event in the pathogenesis of several neurodegenerative diseases (6–15,17,21). In HD, the CASP6-generated 586aa HTT fragment is observed in affected brain regions, and a murine model expressing the 586aa mutant HTT fragment develops neurological abnormalities similar to those observed in HD mouse models (6,103). CASP6-cleaved APP fragments are observed early in human AD brain (104), and processing of APP at this site generates a small peptide that is a potent inducer of apoptosis (97). In addition to APP, cleavage of several CASP6 substrates has been detected in human AD brain (48,105,106). As an example, p97, a valosin containing ubiquitin-dependent ATPase, is cleaved by CASP6 in AD brain, and the resultant fragment impairs the proteasome and destabilizes endogenous p97 (48). Importantly, CASP6-cleaved tau (17,107) and CASP6-cleaved p97 (48) are detected in mild cognitive impaired and AD human brains, suggesting that the activity of CASP6 precedes the clinical and pathological diagnosis of AD. Of interest, CASP6-cleaved tau is observed in AD and HD brains (15,17). Of note, inhibiting CASP6 cleavage of APP provides some protection *in vivo* against AD-like phenotype (9–13,108) and eliminating cleavage at the 586aa CASP6 site of mutant HTT (C6R) is sufficient to preserve neuropathological deficits and behavioral disturbances in a murine model of HD (6–8,15,43), making CASP6 a potential target for therapeutic intervention in neurodegenerative diseases. The fact that the proform of CASP6 only interacts with the 513aa WT htt fragment and not with the mhtt fragment suggests that WT htt may attenuate CASP6 activation, but that mhtt is no longer able to perform this function. This notion is in line with the well-established neuroprotective properties of WT htt. Indeed, although the mechanism(s) underlying the neuroprotective function of htt is poorly defined, a role for htt as a caspase inhibitor has been demonstrated (109,110). It is interesting to speculate whether the loss of interaction between the proform of casp6 and mutant htt may contribute to the increased CASP6 activation in HD.

To identify CASP6 interactors of high interest and their relationship to the disease state, we assessed our high-confidence list of CASP6 interactors to determine whether any show alterations in HD human brain using microarray data sets published previously (84,85). Interestingly, a significant number show alterations in HD human brain. Of the potential interactors showing alterations, we observe an over-representation of the insulin/IGF pathway-protein kinase B signaling cascade, p53 and PI3

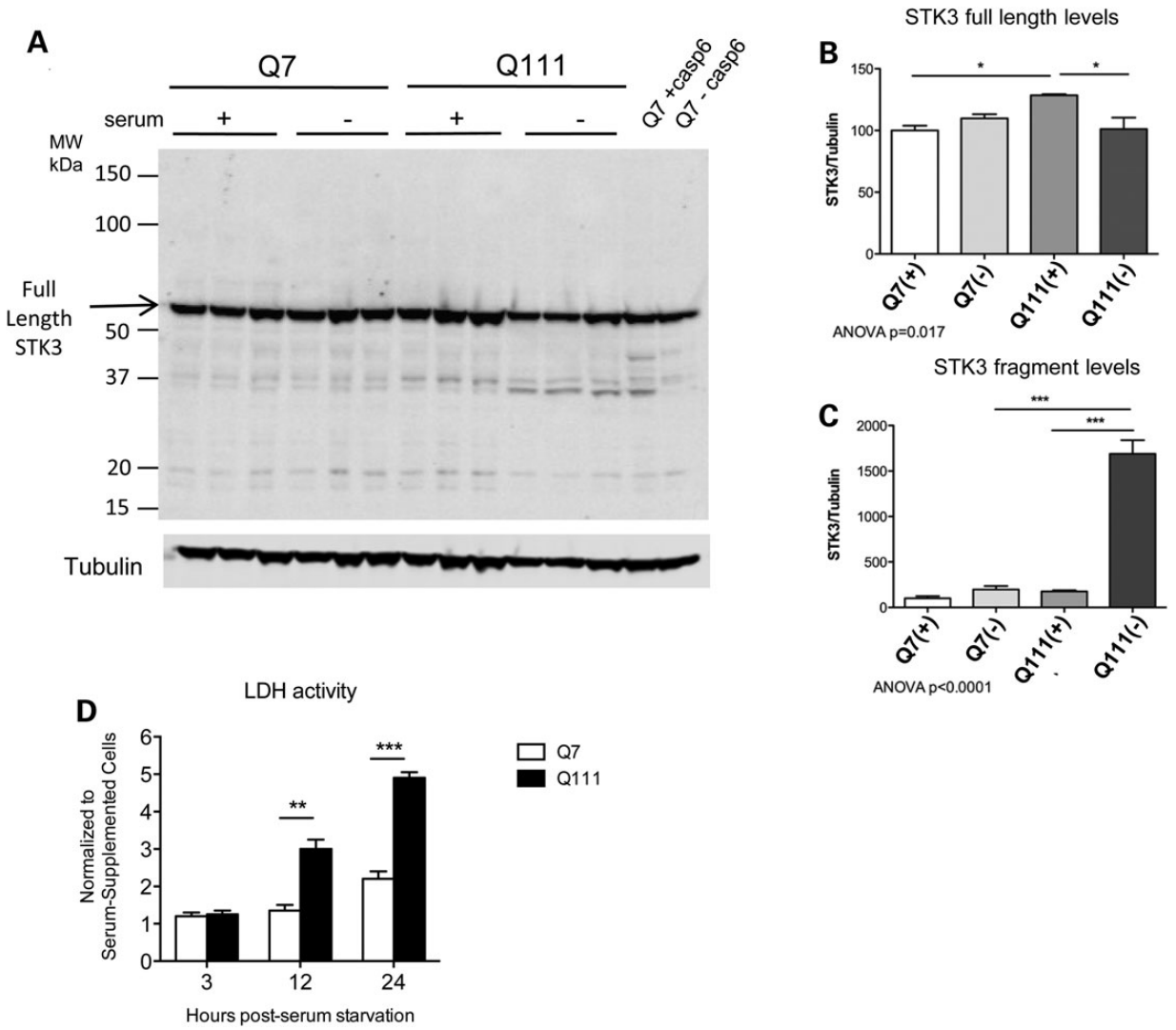

Figure 6. Alterations in expression levels and post-translational modifications of STK3 observed in acute and chronic models of HD. (**A**) Immortalized striatal cells with ($STHdh^{Q111}$) and without ($STHdh^{Q7}$) mutant HTT were incubated ± serum and using western blotting assessed at 24 h after starvation for protein expression of STK3 ($n = 3$). Controls include $STHdh^{Q7}$ lysate ± CASP6. (**B**) A significant increase in FL levels of the pro-apoptotic kinase, STK3, is observed in striatal cells expressing mutant HTT compared with WT at baseline [ANOVA $P < 0.017$, *post hoc* $STHdh^{Q7}$(+) versus $STHdh^{Q111}$(+) $P < 0.05$]. In contrast, FL levels of STK3 are decreased in $STHdh^{Q111}$(–) when compared with $STHdh^{Q111}$(+) cells (*post hoc* $P < 0.05$) as expected due to the cleavage of STK3. (**C**) A significant increase in fragment levels of STK3 is observed in cells expressing mutant HTT compared with WT after serum starvation [ANOVA $P < 0.0001$, *post hoc* $STHdh^{Q7}$(–) versus $STHdh^{Q111}$(–) $P < 0.001$]. (**D**) Evaluation of cell death in serum-starved $STHdh^{Q7}$ and $STHdh^{Q111}$ cells demonstrates that a significant increase in cell death is observed in $STHdh^{Q111}$ cells 12 and 24 h after starvation. Tubulin was used as a loading control.

kinase pathways. There are a number of proteins in common in these pathways including PDPK1, P13K3R1, PTEN, AKT and p53, all of which are implicated in the pathogenesis of HD (92,111–116). P53, a direct regulator of CASP6 (117), is a key protein involved in the cellular stress response and the p53 pathway connected by numerous negative and positive feedback loops including Wnt-beta-catenin, IGF-1-AKT, Rb-E2F, p38 MAP kinase, cyclin-cdk, p14/19 ARF pathways and cyclin G-PP2A and p73 gene products (reviewed in 118). The PI3 kinase pathway is also involved in several key biological processes including survival, metabolism and gene regulation (reviewed in 119).

We identified and validated several novel CASP6 substrates. DAXX has been previously implicated in stroke-mediated cell death and originally identified as a protein that binds to the death domain of the receptor FAS and potentiates FAS-induced apoptosis (120). Cleavage fragments of DAXX are pro-apoptotic and activate the JNK pathway in an *in vitro* model (121). Multiple functions have been described including a role as a potent transcription repressor that binds to sumoylated transcription factors and as a suppressor of the neuroprotective protein kinase B (AKT) signaling pathway. Activation of CASP6 and increases in DAXX are observed in a high-glucose-induced apoptosis model (122). Cleavage of DAXX would interfere with its interaction with histone 3.3 due to disruption of its histone-binding domain and may lead to alterations in the deposition of histones on DNA and cause chromatin condensation. Proof of principle studies reveals a marked reduction in infarct size and apoptosis in ischemia-induced cell death with knockdown and/or expression of a dominant-negative form of DAXX (120,123). DAXX is also implicated in AD-mediated cell death (120). Of significance, robust increases in DAXX mRNA are observed in human AD brain (124,125). DAXX destabilizes ASK1 causing release of GRX1 and

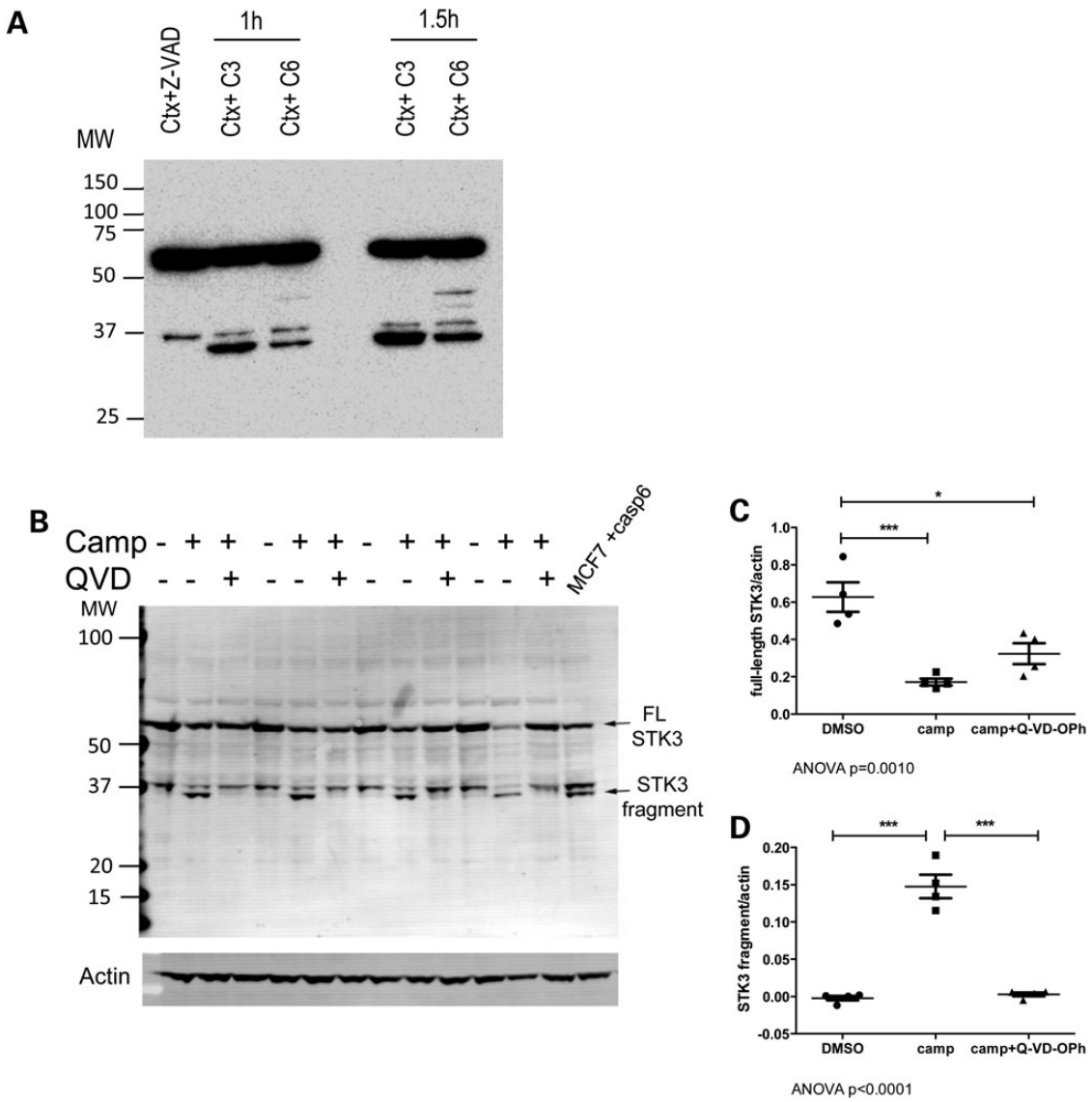

Figure 7. Cleavage of STK3 in the absence of caspase-3. Alterations in expression levels and post-translational modifications of STK3 are observed in stressed MCF7 cells. (**A**) Incubation of murine cortex with either recombinant casp3 or CASP6 demonstrates that both caspase-3 and caspase-6 cleave STK3. However, caspase-3 generates a single cleavage fragment, whereas in contrast, caspase-6 generates three cleavage fragments of STK3. In addition, (**B**) western blotting demonstrates that MCF7 cells, which lack caspase-3, stressed with camptothecin show a decrease in FL STK3 levels and an increase in STK3 fragments compared with unstressed MCF7 cells. (**C**) A significant decrease in FL levels of STK3 is observed in MCF7 cells after camptothecin stress ($n = 4$, $P < 0.001$). (**D**) Furthermore, a significant increase in STK3 fragment levels is observed in MCF7 cells after stress ($n = 4$, $P < 0.001$). In contrast, the STK3 fragment was not detected in stressed MCF7 cells pre-treated with the pan caspase inhibitor Q-VD-OPh. Actin was used as a loading control.

TRX1, redox proteins that are involved in stabilizing ASK1 and inhibiting the DAXX-ASK1-JNK toxic cell death pathway. Decreased protein expression of TRX1 is observed in human AD cortex and hippocampus, and overexpression of TRX1 in a cellular model of AD protects against Aß toxicity (126). A diagram of DAXX protein showing structural (coiled coil) and nuclear localization signal (NLS) motifs, and predicted CASP6 recognition sites, is included as an example (Fig. 5B). Strikingly, the predicted CASP6 recognition sites cluster around the structural and signaling motifs.

Validated substrates also include RBM17 and USP32. Cleavage of RBM17, a protein involved in the splicesomal complex, may interfere with its function in mRNA splicing, thereby altering the regulation of alternative slicing on a global scale. As an example, the U2A-F homology motif, present in RBM17, mediates PPIs between factors involved in constitutive RNA splicing (127). Through this domain, RBM17 regulates alternative splicing of the apoptosis regulatory gene FAS, a key player in PCD pathways. Importantly, splicing of FAS determines whether it encodes a pro-apoptotic or anti-apoptotic form of the FAS protein. RBM17 induces exon skipping of FAS, resulting in the production of the anti-apoptotic form (127). Significantly, *in vitro*-generated fragments of RBM17 cannot bind an AG-containing RNA ligand (127). CASP6 cleavage of RBM17 may provide the mechanism whereby decreased regulation of FAS through RBM17 causes a shift toward production of the pro-apoptotic form of FAS. USP32 is an ubiquitin protease and Ca^{++} binding protein known to be involved in protein degradation. *In vitro*-generated fragments of USP32 have been shown to have alternate subcellular localizations, suggesting possible alternate functions of the protein fragments (128).

A number of serine–threonine kinases play important roles in programmed cell death pathways, and caspase cleavage of STK3 and STK4 is a known mechanism underlying amplification of the apoptotic response (90,129,130). Indeed, evolutionary conserved caspase sites in STK3 and STK4 hint at important biological roles for the fragments generated. Furthermore, STK3 and STK4 contain NES and NLS sequences (131), suggesting that cleavage by caspases may alter the subcellular localization, substrate specificity and/or protein interactions of the fragments when compared with the parent protein. CASP3 has been previously been shown to cleave STK3 and STK4 and CASP6 shown to cleave STK4 (90,129,130). Of note, particular fragments of STK4 demonstrate distinct catalytic activity and the function of fragments (pro-apoptotic) differ from that of the parent protein (89,90). Specifically, caspase cleavage removes the inhibitory C-terminal domain, and the N-terminal fragment is transported to the nucleus. Importantly, in the context of the pathogenesis of HD, IGF-1 inhibits STK3 cleavage and kinase activity via the PI3K/AKT pathway (91). Once STK3 kinase activity is activated via caspase cleavage (cleavage converts STK3 into constitutively active kinase), phosphorylation of c-Jun, H2B, JNK and p38 occurs and STK3 fragments localize to the nucleus prior to DNA fragmentation, suggesting additional nuclear functions of the STK3 fragments in apoptosis. STK3 is only the third kinase shown to interact with CASP6 (132,133). However, in general, caspases are targets of kinases and phosphatases, which facilitate exquisite calibration of caspase activation (134). Conversely, kinases can be targets of caspases, as in the case of RIPK1 and CASP6 (132), leading to inactivation of the kinase and termination of specific signaling pathways.

The evidence demonstrating CASP6 activation and cleavage of HTT and tau in HD mouse models, but not in the caspase-6-resistant HD mice (15), suggests that proteolysis of CASP6 substrates and generation of fragments play a crucial role in the amplification of CASP6 activity and neurotoxic signaling in HD. In both HD and AD, alterations in AKT [a substrate of CASP6 (135)], including decreased expression and cleavage fragments, are observed, suggesting that decreased phosphorylation of STK3 may occur (136,137). Furthermore, a decrease in IGF-1, a potent upstream activator of AKT, has also been reported in a cellular model of HD and may contribute to the downstream alterations in AKT and consequent effects (138). Microarray studies demonstrate that STK3 mRNA is significantly increased in early grade human HD brain (84). We demonstrate here that alterations in STK3 protein expression levels and post-translational modifications are detected in a cellular model of HD and caspase-mediated generation of STK3 fragments observed under conditions of stress in cells expressing mhtt. CASP6 now links STK3 and DAXX with AKT, JNK and histones in the pathogenesis of neurological disorders and highlights an early role for these substrates in neurodegenerative pathways.

In conclusion, we have identified novel members of the CASP6 interactome and demonstrate that a number of these interactors are involved in key signaling pathways observed in neurodegenerative diseases. These data will empower future investigations into the role of caspases in neurodegenerative diseases and their potential as targets for therapeutic intervention.

Materials and Methods

Yeast two-hybrid assay

To create a prey matrix for interaction mating, the MATα yeast strain L40ccα was individually transformed with pACT4-DM-based plasmids encoding prey proteins. The resulting yeast clones were arrayed in 384-well microtiter plates. cDNA fragments encoding the bait protein fragments (CASP6_p10, CASP6_p20 and CASP6_p34) were subcloned into the yeast expression vector pBTM116-D9, and the resulting plasmids were transformed into the MATa yeast strain L40ccua. The activation of the reporter genes *HIS3*, *URA3* and lacZ in autoactivation tests as a result of the production of bait proteins was tested systematically. All three bait constructs were non-autoactive and were taken for interaction mating assays with prey proteins (139). Liquid cultures of MATα yeast strains (preys) were replicated in 384-well microtiter plates using a pipetting robot (Tecan, Freedom EVOware®, Switzerland) and then mixed with bait protein producing MATa strains. For interaction mating, yeast mixtures were transferred onto YPD agar plates using a spotting robot (K4, KBiosystems, England) and incubated for 48 h at 30°C. After mating, clones were automatically picked from agar plates and transferred into 384-well microtiter plates containing SDII (-Leu-Trp) liquid medium, and from there, they were spotted onto SDII (-Leu-Trp) agar to select for diploid yeasts carrying both bait and prey vectors. After incubation for 48 h at 30°C, diploid yeast clones were spotted onto SDIV (-Leu-Trp-Ura-His) agar to detect positive PPIs as well as on high-density nylon membranes on top of SDIV agar plates for a LacZ assay. In the lacZ assay, ß-galactosidase is produced just in growing cells in which bait and prey proteins interact. After incubation for 3–4 days at 30°C, grown colonies were fractured with liquid nitrogen, and ß-galactosidase activity was detected using the X-Gal substrate. Digital images were taken from agar plates as well as from high-density nylon membranes for Visual Grid software (GPC Biotech, Germany)-assisted result digitalization. The automated Y2H screen was done in four repetitions.

LUMIER assay

For LUMIER assays, protein A (PA)–Renilla luciferase (RL)-tagged fusion proteins were co-produced with firefly luciferase (FL)-tagged putative interactor proteins in HEK293 cells. After 48 h, protein complexes were co-immunoprecipitated from cell extracts with IgG-coated magnetic beads (Dynabeads®; Invitrogen, USA); interactions between bait (PA–RL fusions) and prey proteins (FL fusions) were monitored by quantification of FL activities (140). Quantification of RL activity was used to confirm that PA–RL-tagged bait proteins are successfully immunoprecipitated from cell extracts. To detect Renilla- and FL-based luminescence in samples with fusion proteins, the Dual-Glo Luciferase Kit (Promega, USA) was used. Bioluminescence was quantified in a luminescence plate reader (TECAN Infinite M1000). For each interaction, both PA–RL and FL interactor fusion combinations were tested. Further on, for each protein pair tested (interaction between selected bait and prey proteins), three different parallel co-immunoprecipitation (Co-IP A–C) experiments were performed in HEK293 cells, in order to assess the specificity of an interaction. To investigate the interaction between the proteins X and Y, the protein pairs (A) PA–RL-X/FL-Y, (B) PA–RL/FL-Y and (C) PA–RL-X/FL were individually co-produced in HEK293 cells. The proteins PA–RL (fusions of PA and RL) and FL in experiments B and C were used as controls to examine background protein binding. The resulting protein complexes in Co-IPs A–C are systematically analyzed by quantification of firefly luciferase activity. R_op and R_ob binding ratios were obtained by dividing the firefly luminescence activity measured in sample A by activities found in samples B and C. These controls work to measure the protein interaction specificity. Low R_op values are an indication for unspecific prey protein interactions, whereas low R_ob values

indicate unspecific bait protein interactions. Based on empirical studies with a set of well-characterized positive and negative interaction pairs (data not shown), we defined that R_op and R_ob binding ratios of >1.5 indicate reliable, specific PPIs.

Prediction of caspase-6 substrates

Interactors were assessed for predicted caspase-6 cleavage sites using the SitePrediction web tool (HTTp://www.dmbr.ugent.be/prx/bioit2-public/SitePrediction/; REF). As SitePrediction requires protein identifiers (IDs) for input, the DAVID gene ID conversion tool (Accessed January 6, 2010; REF) was used to convert Entrez Gene IDs or GenBank IDs to Refseq protein IDs. The 87 interactors were mapped to 135 Refseq IDs because each gene may map to one or more protein isoforms. These were submitted to SitePrediction (Accessed January 7, 2010) using the 'caspase-6_Homo_sapiens_4_2' cleavage model based on known human caspase-6 cleavage sites in the Merops database. Default parameters were used with the 'extended statistics' setting and a threshold of 70. An interactor was considered a putative caspase-6 substrate if at least one cleavage site was predicted with 99.9% specificity.

Identification of HTT-CASP6-shared interactors

To determine which caspase-6 Y2H interactors are known HTT interactors, we compared to HTT interactor publications (141–143).

Genes dysregulated in human HD brain

Direct interaction partners of CASP6 identified by the Y2H screen or known from the literature were identified as potentially perturbed in HD using a three-step expression data-filtering strategy. Gene expression analysis was carried out using the open source R software packages, available as part of the BioConductor project (www.bioconductor.org). The Gene Atlas data set was normalized using MAS5 (Affymetrix Microarray Suite 5). False discovery rate values were computed using the local pooled error approach to identify significantly expressed genes (144). For the detection of dysregulated genes, we computed empirical Bayes moderated t-statistics, which corrects gene expression for the collection site, gender and age. For the three filtering steps, we used two publicly available gene expression data sets [Gene Atlas (84,145)]. In the first filtering step, 21 of 121 CASP6 interactors were identified as being differentially expressed (adjusted $P < 0.00001$) in human brain compared with non-brain tissues (adrenal gland, heart, kidney, liver, lung, lymph node, muscle, prostate, pancreas, placenta, salivary gland, thymus, thyroid, tonsil, testis, trachea, uterus and uterine corpus) using the Gene Atlas data set (145). As pathogenesis in HD is brain-region-specific with neurons in the basal ganglia most severely affected (31), we next analyzed the 21 brain-specific CASP6 interactors for being differentially expressed (adjusted $P < 0.001$) in the CN when compared with the motor cortex, prefrontal cortex and the cerebellum (84). Fifteen brain-specific interactors of CASP6 were also differentially expressed in the CN. Finally, the CN-specific CASP6 interactors were filtered for genes differentially expressed in the CN of HD patient brains and healthy individuals. To define differentially expressed genes, expression profiles of brains of 44 HD patients and 36 healthy individuals were analyzed (84,85). Only genes with $P < 0.001$ were accepted as being differentially expressed in HD patients compared with controls. Using this step-by-step approach, the CN-specific HD network with six potentially dysregulated CASP6 interaction partners was predicted.

Caspase-6 cleavage assays

Five samples, each 30 µg of WT murine cortex protein lysates, were incubated with 0 nM, 30 nM, 300 nM, 3 µM or 30 µM of CASP6 (Enzo Life Sciences, USA) at 37°C for 1 h; another four samples (30 µg of WT cortex lysate) were incubated with 15 µM CASP6 at 37°C for 5, 15, 30 or 60 min. Samples were then used for western blotting as described subsequently.

Cell culture and LDH assay

Immortalized striatal neuronal cell lines STHdh^{Q7} and STHdh^{Q111} were cultured at 33°C in Dulbecco's modified Eagle's medium (DMEM, Gibco, USA) supplemented with 10% fetal bovine serum, 100× penicillin/streptomycin (Gibco), 2 mM L-glutamine (Gibco) and 0.5 mg/ml active G418. Cells were grown in a humidified atmosphere containing 5% CO_2 and harvested using 0.25% trypsin-EDTA. For serum deprivation experiments, 600 000 cells were seeded on day 1, medium was changed to serum-free media on day 2 and cells harvested after 24 h of starvation. MCF-7 cells were cultured in DMEM supplemented with 10% fetal calf serum and 2 mM L-glutamine. Cells were stressed with 5 µM camptothecin for 16 h in the presence or absence of the caspase inhibitor Q-VD-OPh (1 mM) and harvested by scraping.

Protein analysis and western blotting

Murine cortical tissue lysates for CASP6 cleavage assays were homogenized in 0.303 M sucrose, 20 mM Tris–HCl pH 7.2, 0.5 mM EDTA and 1 mM $MgCl_2$, without protease inhibitors using a glass-teflon IKA-RW 15 homogenizer (Tekmar Company, USA) at maximum speed and cleared by centrifugation for 5 min at 1300*g*. Lysates were then run on sodium dodecyl sulfate–polyacrylamide gel electrophoresis and probed with one of the following antibodies: DAXX (Santa Cruz, USA: sc-7152) at 1:200, STK3 (Abcam, UK: ab52641) at 1:2000, PI3RK1 (Abcam: ab90578) at 1:920, PALMD (ProteinTech Group, USA: 16531-1-AP) at 1:800, USP32 (Abcam: ab86792) at 1:2000, RBM17 (ProteinTech Group: 13918-1-AP) at 1:1200, GSK-3α/β (Santa Cruz: sc-7291) at 1:500, BAIAP2 (ProteinTech Group: 11087-2-AP) at 1:2000, STX16 (ProteinTech) at 1:500 and Actin (Sigma) at 1:1000. Three additional RBM17 antibodies demonstrate an ~70 kDa band on the datasheet (ProteinTech Group: 15374-1-AP, GeneTex: GTX120047 and Abcam: ab101441). Cell lysates from immortalized striatal cultures were lysed in single detergent phosphatase lysis buffer including protease inhibitors (50 mM Tris pH 8.0, 150 mM NaCl, 1% Igepal/NP-40, 40 mM B-gp, 10 mM NaF, 1 mM NaVan, 1 mM PMSF, 5 µM zVAD and 1× Roche Complete). Protein concentration was measured by the DC protein assay kit (Bio Rad, USA). Lysates were then separated on 4–12% Bis–Tris gels (Invitrogen). Following transfer, membranes were probed with the STK3 antibody and beta-tubulin (1:5000; T4026, Sigma-Aldrich, USA). Cell pellets from MCF-7 cultures were lysed in 50 mM HEPES pH 7.4, 100 mM NaCl, 1% Igepal, 1 mM EDTA and 10% glycerol with 4.2 µM Pefabloc and 'Complete' protease inhibitor cocktail (Roche, Switzerland) and protein concentrations determined. Following transfer, the membrane was probed with anti-STK3 and anti-Actin antibodies. All immunoblots were prepared following standard procedures and used infrared-labeled secondary antibodies (1:5000; Rockland, USA), Immobilon-PVDF-FL membranes and the Li-Cor Odyssey Infrared imaging system (BioSciences, USA). Quantitative analysis of immunoblotting was based on the integrated intensity from Li-Cor Odyssey software (v2.0). To assess serum starvation-induced cell death in STHdh^{Q7} and STHdh^{Q111}, cells were seeded at 10 000 cells/well in a 96-well

plate in complete media. After 24 h, serum starvation was induced by removing the complete media, washing once with phosphate-buffered saline and adding serum-free media. Control (non-serum-starved) cells received fresh complete media. Twenty-four hours later, media were collected and centrifuged at 2800 rpm for 4 min at 4°C to remove any cell debris, and the supernatant was collected for LDH activity measurements. The LDH assay was performed according to the manufacturer's instructions (Roche Cytotoxicity Detection Kit).

Statistical analysis

Except where noted otherwise, statistical analysis was performed using one-way and two-way ANOVA (in the case of significant effect of genotype, *post hoc* comparisons between genotypes were performed using Bonferroni). *P*-values, SEM, means and standard deviations were calculated using GraphPad Prism version 6.0. Differences between means were considered to be statistically significant if $P < 0.05$.

Supplementary Material

Supplementary material is available at *HMG* online.

Conflict of Interest statement. The authors confirm that there is no conflict of interest.

Funding

This work was supported by the Canada Research Chair funding (R.K.G. and M.R.H.) and by grants from the Canadian Institute of Health Research (M.R.H.) and from BMBF (NGFN-Plus; NeuroNet, 01GS08169-73; MooDS, 01GS08150; Mutanom, 01GS08108; GoBio), EU (EuroSpin, Health-F2-2009-241498 and SynSys, HEALTH-F2-2009-242167) and the Helmholtz Association (MSBN, HelMA, HA-215) to E.E.W. M.A.P. is supported by a Strategic Positioning Fund for Genetic Orphan Diseases from the Agency for Science Technology and Research and the National University of Singapore. N.S. is supported by a Canadian Institute of Health Research postdoctoral salary award. M.R.H. is a Killam University Professor and holds a Canada Research Chair in Human Genetics. R.K.G. holds a Canada Research Chair in Neurodegenerative diseases.

References

1. Graham, R.K., Ehrnhoefer, D.E. and Hayden, M.R. (2011) Caspase-6 and neurodegeneration. *Trends Neurosci.*, **34**, 646–656.
2. Okouchi, M., Ekshyyan, O., Maracine, M. and Aw, T.Y. (2007) Neuronal apoptosis in neurodegeneration. *Antioxid. Redox Signal.*, **9**, 1059–1096.
3. Friedlander, R.M. (2003) Apoptosis and caspases in neurodegenerative diseases. *N. Engl. J. Med.*, **348**, 1365–1375.
4. Elmore, S. (2007) Apoptosis: a review of programmed cell death. *Toxicol. Pathol.*, **35**, 495–516.
5. Obexer, P. and Ausserlechner, M.J. (2014) X-linked inhibitor of apoptosis protein—a critical death resistance regulator and therapeutic target for personalized cancer therapy. *Front. Oncol.*, **4**, 197.
6. Graham, R.K., Deng, Y., Slow, E.J., Haigh, B., Bissada, N., Lu, G., Pearson, J., Shehadeh, J., Bertram, L., Murphy, Z. *et al.* (2006) Cleavage at the caspase-6 site is required for neuronal dysfunction and degeneration due to mutant huntingtin. *Cell*, **125**, 1179–1191.
7. Pouladi, M.A., Graham, R.K., Karasinska, J.M., Xie, Y., Santos, R.D., Petersen, A. and Hayden, M.R. (2009) Prevention of depressive behaviour in the YAC128 mouse model of Huntington disease by mutation at residue 586 of huntingtin. *Brain*, **32**, 919–932.
8. Milnerwood, A.J., Gladding, C.M., Pouladi, M.A., Kaufman, A. M., Hines, R.M., Boyd, J.D., Ko, R.W., Vasuta, O.C., Graham, R. K., Hayden, M.R. *et al.* (2010) Early increase in extrasynaptic NMDA receptor signaling and expression contributes to phenotype onset in Huntington's disease mice. *Neuron*, **65**, 178–190.
9. Galvan, V., Gorostiza, O.F., Banwait, S., Ataie, M., Logvinova, A.V., Sitaraman, S., Carlson, E., Sagi, S.A., Chevallier, N., Jin, K. *et al.* (2006) Reversal of Alzheimer's-like pathology and behavior in human APP transgenic mice by mutation of Asp664. *Proc. Natl Acad. Sci. USA*, **103**, 7130–7135.
10. Saganich, M.J., Schroeder, B.E., Galvan, V., Bredesen, D.E., Koo, E.H. and Heinemann, S.F. (2006) Deficits in synaptic transmission and learning in amyloid precursor protein (APP) transgenic mice require C-terminal cleavage of APP. *J. Neurosci.*, **26**, 13428–13436.
11. Galvan, V., Zhang, J., Gorostiza, O.F., Banwait, S., Huang, W., Ataie, M., Tang, H. and Bredesen, D.E. (2008) Long-term prevention of Alzheimer's disease-like behavioral deficits in PDAPP mice carrying a mutation in Asp664. *Behav. Brain Res.*, **191**, 246–255.
12. Banwait, S., Galvan, V., Zhang, J., Gorostiza, O.F., Ataie, M., Huang, W., Crippen, D., Koo, E.H. and Bredesen, D.E. (2008) C-terminal cleavage of the amyloid-beta protein precursor at Asp664: a switch associated with Alzheimer's disease. *J. Alzheimers Dis.*, **13**, 1–16.
13. Nguyen, T.V., Galvan, V., Huang, W., Banwait, S., Tang, H., Zhang, J. and Bredesen, D.E. (2008) Signal transduction in Alzheimer disease: p21-activated kinase signaling requires C-terminal cleavage of APP at Asp664. *J. Neurochem.*, **104**, 1065–1080.
14. Young, J.E., Gouw, L., Propp, S., Sopher, B.L., Taylor, J., Lin, A., Hermel, E., Logvinova, A., Chen, S.F., Chen, S. *et al.* (2007) Proteolytic cleavage of ataxin-7 by caspase-7 modulates cellular toxicity and transcriptional dysregulation. *J. Biol. Chem.*, **282**, 30150–30160.
15. Graham, R.K., Deng, Y., Carroll, J., Vaid, K., Cowan, C., Pouladi, M.A., Metzler, M., Bissada, N., Wang, L., Faull, R.L. *et al.* (2010) Cleavage at the 586 amino acid caspase-6 site in mutant huntingtin influences caspase-6 activation *in vivo*. *J. Neurosci.*, **30**, 15019–15029.
16. Albrecht, S., Bogdanovic, N., Ghetti, B., Winblad, B. and LeBlanc, A.C. (2009) Caspase-6 activation in familial Alzheimer disease brains carrying amyloid precursor protein or presenilin I or presenilin II mutations. *J. Neuropathol. Exp. Neurol.*, **68**, 1282–1293.
17. Albrecht, S., Bourdeau, M., Bennett, D., Mufson, E.J., Bhattacharjee, M. and LeBlanc, A.C. (2007) Activation of caspase-6 in aging and mild cognitive impairment. *Am. J. Pathol.*, **170**, 1200–1209.
18. Harrison, D.C., Davis, R.P., Bond, B.C., Campbell, C.A., James, M.F., Parsons, A.A. and Philpott, K.L. (2001) Caspase mRNA expression in a rat model of focal cerebral ischemia. *Brain Res. Mol. Brain Res.*, **89**, 133–146.
19. Singh, A.B., Kaushal, V., Megyesi, J.K., Shah, S.V. and Kaushal, G.P. (2002) Cloning and expression of rat caspase-6 and its localization in renal ischemia/reperfusion injury. *Kidney Int.*, **62**, 106–115.
20. Ferrer, I., Lopez, E., Blanco, R., Rivera, R., Krupinski, J. and Marti, E. (2000) Differential c-Fos and caspase expression

following kainic acid excitotoxicity. *Acta Neuropathol.*, **99**, 245–256.
21. Mookerjee, S., Papanikolaou, T., Guyenet, S.J., Sampath, V., Lin, A., Vitelli, C., DeGiacomo, F., Sopher, B.L., Chen, S.F., La Spada, A.R. *et al.* (2009) Posttranslational modification of ataxin-7 at lysine 257 prevents autophagy-mediated turnover of an N-terminal caspase-7 cleavage fragment. *J. Neurosci.*, **29**, 15134–15144.
22. Taghibiglou, C., Martin, H.G., Lai, T.W., Cho, T., Prasad, S., Kojic, L., Lu, J., Liu, Y., Lo, E., Zhang, S. *et al.* (2009) Role of NMDA receptor-dependent activation of SREBP1 in excitotoxic and ischemic neuronal injuries. *Nat. Med.*, **15**, 1399–1406.
23. Aarts, M., Liu, Y., Liu, L., Besshoh, S., Arundine, M., Gurd, J.W., Wang, Y.T., Salter, M.W. and Tymianski, M. (2002) Treatment of ischemic brain damage by perturbing NMDA receptor- PSD-95 protein interactions. *Science*, **298**, 846–850.
24. Chen, M., Ona, V.O., Li, M., Ferrante, R.J., Fink, K.B., Zhu, S., Bian, J., Guo, L., Farrell, L.A., Hersch, S.M. *et al.* (2000) Minocycline inhibits caspase-1 and caspase-3 expression and delays mortality in a transgenic mouse model of Huntington disease. *Nat. Med.*, **6**, 797–801.
25. Ona, V.O., Li, M., Vonsattel, J.P., Andrews, L.J., Khan, S.Q., Chung, W.M., Frey, A.S., Menon, A.S., Li, X.J., Stieg, P.E. *et al.* (1999) Inhibition of caspase-1 slows disease progression in a mouse model of Huntington's disease. *Nature*, **399**, 263–267.
26. Peng, J., Wu, Z., Wu, Y., Hsu, M., Stevenson, F.F., Boonplueang, R., Roffler-Tarlov, S.K. and Andersen, J.K. (2002) Inhibition of caspases protects cerebellar granule cells of the weaver mouse from apoptosis and improves behavioral phenotype. *J. Biol. Chem.*, **277**, 44285–44291.
27. Rampon, C., Jiang, C.H., Dong, H., Tang, Y.P., Lockhart, D.J., Schultz, P.G., Tsien, J.Z. and Hu, Y. (2000) Effects of environmental enrichment on gene expression in the brain. *Proc. Natl Acad. Sci. USA*, **97**, 12880–12884.
28. Nakamura, H., Kobayashi, S., Ohashi, Y. and Ando, S. (1999) Age-changes of brain synapses and synaptic plasticity in response to an enriched environment. *J. Neurosci. Res.*, **56**, 307–315.
29. Jiang, C.H., Tsien, J.Z., Schultz, P.G. and Hu, Y. (2001) The effects of aging on gene expression in the hypothalamus and cortex of mice. *Proc. Natl Acad. Sci. USA*, **98**, 1930–1934.
30. The Huntington's Disease Collaborative Research Group (1993) A novel gene containing a trinucleotide repeat that is expanded and unstable on Huntington's disease chromosomes.. *Cell*, **72**, 971–983.
31. Vonsattel, J.P., Myers, R.H., Stevens, T.J., Ferrante, R.J., Bird, E.D. and Richardson, E.P. Jr (1985) Neuropathological classification of Huntington's disease. *J. Neuropathol. Exp. Neurol.*, **44**, 559–577.
32. Beal, M.F., Ferrante, R.J., Swartz, K.J. and Kowall, N.W. (1991) Chronic quinolinic acid lesions in rats closely resemble Huntington's disease. *J. Neurosci.*, **11**, 1649–1659.
33. Graveland, G.A., Williams, R.S. and DiFiglia, M. (1985) Evidence for degenerative and regenerative changes in neostriatal spiny neurons in Huntington's disease. *Science*, **227**, 770–773.
34. Landwehrmeyer, G.B., Standaert, D.G., Testa, C.M., Penney, J.B. Jr and Young, A.B. (1995) NMDA receptor subunit mRNA expression by projection neurons and interneurons in rat striatum. *J. Neurosci.*, **15**, 5297–5307.
35. Ferrante, R.J., Kowall, N.W. and Richardson, E.P. Jr (1991) Proliferative and degenerative changes in striatal spiny neurons in Huntington's disease: a combined study using the section-Golgi method and calbindin D28k immunocytochemistry. *J. Neurosci.*, **11**, 3877–3887.
36. McGeer, E.G. and McGeer, P.L. (1976) Duplication of biochemical changes of Huntington's chorea by intrastriatal injections of glutamic and kainic acids. *Nature*, **263**, 517–519.
37. Zeron, M.M., Hansson, O., Chen, N., Wellington, C.L., Leavitt, B.R., Brundin, P., Hayden, M.R. and Raymond, L.A. (2002) Increased sensitivity to N-methyl-D-aspartate receptor-mediated excitotoxicity in a mouse model of Huntington's disease. *Neuron*, **33**, 849–860.
38. Graham, R.K., Slow, E.J., Deng, Y., Bissada, N., Lu, G., Pearson, J., Shehadeh, J., Leavitt, B.R., Raymond, L.A. and Hayden, M. R. (2006) Levels of mutant huntingtin influence the phenotypic severity of Huntington disease in YAC128 mouse models. *Neurobiol. Dis.*, **21**, 444–455.
39. Parameshwaran, K., Dhanasekaran, M. and Suppiramaniam, V. (2008) Amyloid beta peptides and glutamatergic synaptic dysregulation. *Exp. Neurol.*, **210**, 7–13.
40. Hynd, M.R., Scott, H.L. and Dodd, P.R. (2004) Glutamate-mediated excitotoxicity and neurodegeneration in Alzheimer's disease. *Neurochem. Int.*, **45**, 583–595.
41. Okamoto, S., Pouladi, M.A., Talantova, M., Yao, D., Xia, P., Ehrnhoefer, D.E., Zaidi, R., Clemente, A., Kaul, M., Graham, R.K. *et al.* (2009) Balance between synaptic versus extrasynaptic NMDA receptor activity influences inclusions and neurotoxicity of mutant huntingtin. *Nat. Med.*, **15**, 1407–1413.
42. Ehrnhoefer, D.E., Wong, B.K. and Hayden, M.R. (2011) Convergent pathogenic pathways in Alzheimer's and Huntington's diseases: shared targets for drug development. *Nat. Rev. Drug Discov.*, **10**, 853–867.
43. Metzler, M., Gan, L., Mazarei, G., Graham, R.K., Liu, L., Bissada, N., Lu, G., Leavitt, B.R. and Hayden, M.R. (2010) Phosphorylation of huntingtin at Ser421 in YAC128 neurons is associated with protection of YAC128 neurons from NMDA-mediated excitotoxicity and is modulated by PP1 and PP2A. *J. Neurosci.*, **30**, 14318–14329.
44. Dix, M.M., Simon, G.M. and Cravatt, B.F. (2008) Global mapping of the topography and magnitude of proteolytic events in apoptosis. *Cell*, **134**, 679–691.
45. Breckenridge, D.G., Stojanovic, M., Marcellus, R.C. and Shore, G.C. (2003) Caspase cleavage product of BAP31 induces mitochondrial fission through endoplasmic reticulum calcium signals, enhancing cytochrome c release to the cytosol. *J. Cell. Biol*, **160**, 1115–1127.
46. Chan, Y.W., Chen, Y. and Poon, R.Y. (2009) Generation of an indestructible cyclin B1 by caspase-6-dependent cleavage during mitotic catastrophe. *Oncogene*, **28**, 170–183.
47. de Calignon, A., Fox, L.M., Pitstick, R., Carlson, G.A., Bacskai, B.J., Spires-Jones, T.L. and Hyman, B.T. (2010) Caspase activation precedes and leads to tangles. *Nature*, **464**, 1201–1204.
48. Halawani, D., Tessier, S., Anzellotti, D., Bennett, D.A., Latterich, M. and LeBlanc, A.C. (2010) Identification of caspase-6-mediated processing of the valosin containing protein (p97) in Alzheimer's disease: a novel link to dysfunction in ubiquitin–proteasome system-mediated protein degradation. *J. Neurosci.*, **30**, 6132–6142.
49. Levkau, B., Scatena, M., Giachelli, C.M., Ross, R. and Raines, E.W. (1999) Apoptosis overrides survival signals through a caspase-mediated dominant-negative NF-kappa B loop. *Nat. Cell Biol.*, **1**, 227–233.
50. Mazars, A., Fernandez-Vidal, A., Mondesert, O., Lorenzo, C., Prevost, G., Ducommun, B., Payrastre, B., Racaud-Sultan, C. and Manenti, S. (2009) A caspase-dependent cleavage of CDC25A generates an active fragment activating cyclin-

dependent kinase 2 during apoptosis. *Cell Death Differ.*, **16**, 208–218.
51. Tang, G., Yang, J., Minemoto, Y. and Lin, A. (2001) Blocking caspase-3-mediated proteolysis of IKKbeta suppresses TNF-alpha-induced apoptosis. *Mol. Cell*, **8**, 1005–1016.
52. Warby, S.C., Doty, C.N., Graham, R.K., Carroll, J.B., Yang, Y.Z., Singaraja, R.R., Overall, C.M. and Hayden, M.R. (2008) Activated caspase-6 and caspase-6-cleaved fragments of huntingtin specifically colocalize in the nucleus. *Hum. Mol. Genet.*, **17**, 2390–2404.
53. Oliver, F.J., de la Rubia, G., Rolli, V., Ruiz-Ruiz, M.C., de Murcia, G. and Murcia, J.M. (1998) Importance of poly(ADP-ribose) polymerase and its cleavage in apoptosis. Lesson from an uncleavable mutant. *J. Biol. Chem.*, **273**, 33533–33539.
54. Wellington, C.L., Singaraja, R., Ellerby, L., Savill, J., Roy, S., Leavitt, B., Cattaneo, E., Hackam, A., Sharp, A., Thornberry, N. *et al.* (2000) Inhibiting caspase cleavage of huntingtin reduces toxicity and aggregate formation in neuronal and nonneuronal cells. *J. Biol. Chem.*, **275**, 19831–19838.
55. Gafni, J., Hermel, E., Young, J.E., Wellington, C.L., Hayden, M. R. and Ellerby, L.M. (2004) Inhibition of calpain cleavage of huntingtin reduces toxicity: accumulation of calpain/caspase fragments in the nucleus. *J. Biol. Chem.*, **279**, 20211–20220.
56. Rao, L., Perez, D. and White, E. (1996) Lamin proteolysis facilitates nuclear events during apoptosis. *J. Cell. Biol.*, **135**, 1441–1455.
57. Charvet, C., Alberti, I., Luciano, F., Jacquel, A., Bernard, A., Auberger, P. and Deckert, M. (2003) Proteolytic regulation of Forkhead transcription factor FOXO3a by caspase-3-like proteases. *Oncogene*, **22**, 4557–4568.
58. Wang, B., Nguyen, M., Breckenridge, D.G., Stojanovic, M., Clemons, P.A., Kuppig, S. and Shore, G.C. (2003) Uncleaved BAP31 in association with A4 protein at the endoplasmic reticulum is an inhibitor of Fas-initiated release of cytochrome c from mitochondria. *J. Biol. Chem.*, **278**, 14461–14468.
59. Lane, J.D., Lucocq, J., Pryde, J., Barr, F.A., Woodman, P.G., Allan, V.J. and Lowe, M. (2002) Caspase-mediated cleavage of the stacking protein GRASP65 is required for Golgi fragmentation during apoptosis. *J. Cell. Biol.*, **156**, 495–509.
60. Walter, J., Schindzielorz, A., Grunberg, J. and Haass, C. (1999) Phosphorylation of presenilin-2 regulates its cleavage by caspases and retards progression of apoptosis. *Proc. Natl Acad. Sci. USA*, **96**, 1391–1396.
61. D'Costa, A.M. and Denning, M.F. (2005) A caspase-resistant mutant of PKC-delta protects keratinocytes from UV-induced apoptosis. *Cell Death Differ.*, **12**, 224–232.
62. Nguyen, M., Breckenridge, D.G., Ducret, A. and Shore, G.C. (2000) Caspase-resistant BAP31 inhibits fas-mediated apoptotic membrane fragmentation and release of cytochrome c from mitochondria. *Mol. Cell. Biol.*, **20**, 6731–6740.
63. Latchoumycandane, C., Anantharam, V., Kitazawa, M., Yang, Y., Kanthasamy, A. and Kanthasamy, A.G. (2005) Protein kinase Cdelta is a key downstream mediator of manganese-induced apoptosis in dopaminergic neuronal cells. *J. Pharmacol. Exp. Ther.*, **313**, 46–55.
64. Assefa, Z., Bultynck, G., Szlufcik, K., Nadif Kasri, N., Vermassen, E., Goris, J., Missiaen, L., Callewaert, G., Parys, J.B. and De Smedt, H. (2004) Caspase-3-induced truncation of type 1 inositol trisphosphate receptor accelerates apoptotic cell death and induces inositol trisphosphate-independent calcium release during apoptosis. *J. Biol. Chem.*, **279**, 43227–43236.
65. Van de Craen, M., Declercq, W., Van den brande, I., Fiers, W. and Vandenabeele, P. (1999) The proteolytic procaspase activation network: an *in vitro* analysis. *Cell Death Differ.*, **6**, 1117–1124.
66. Slee, E.A., Harte, M.T., Kluck, R.M., Wolf, B.B., Casiano, C.A., Newmeyer, D.D., Wang, H.G., Reed, J.C., Nicholson, D.W., Alnemri, E.S. *et al.* (1999) Ordering the cytochrome c-initiated caspase cascade: hierarchical activation of caspases-2, -3, -6, -7, -8, and -10 in a caspase-9-dependent manner. *J. Cell Biol.*, **144**, 281–292.
67. Cowling, V. and Downward, J. (2002) Caspase-6 is the direct activator of caspase-8 in the cytochrome c-induced apoptosis pathway: absolute requirement for removal of caspase-6 prodomain. *Cell Death Differ.*, **9**, 1046–1056.
68. Ramcharitar, J., Afonso, V.M., Albrecht, S., Bennett, D.A. and LeBlanc, A.C. (2013) Caspase-6 activity predicts lower episodic memory ability in aged individuals. *Neurobiol. Aging*, **34**, 1815–1824.
69. LeBlanc, A.C., Ramcharitar, J., Afonso, V., Hamel, E., Bennett, D. A., Pakavathkumar, P. and Albrecht, S. (2014) Caspase-6 activity in the CA1 region of the hippocampus induces age-dependent memory impairment. *Cell Death Differ.*, **21**, 696–706.
70. Gafni, J., Papanikolaou, T., Degiacomo, F., Holcomb, J., Chen, S., Menalled, L., Kudwa, A., Fitzpatrick, J., Miller, S., Ramboz, S. *et al.* (2012) Caspase-6 activity in a BACHD mouse modulates steady-state levels of mutant huntingtin protein but is not necessary for production of a 586 amino acid proteolytic fragment. *J. Neurosci.*, **32**, 7454–7465.
71. Wong, B.K., Ehrnhoefer, D.E., Graham, R.K., Martin, D.D., Ladha, S., Uribe, V., Stanek, L.M., Franciosi, S., Qiu, X., Deng, Y. *et al.* (2015) Partial rescue of some features of Huntington disease in the genetic absence of caspase-6 in YAC128 mice. *Neurobiol. Dis.*, **76**, 24–36.
72. Aharony, I., Ehrnhoefer, D.E., Shruster, A., Qiu, X., Franciosi, S., Hayden, M.R. and Offen, D. (2015) A Huntingtin-based peptide inhibitor of caspase-6 provides protection from mutant Huntingtin-induced motor and behavioral deficits. *Hum. Mol. Genet.*, **24**, 2604–2614.
73. Guyenet, S.J., Mookerjee, S.S., Lin, A., Custer, S.K., Chen, S.F., Sopher, B.L., La Spada, A.R. and Ellerby, L.M. (2015) Proteolytic cleavage of ataxin-7 promotes SCA7 retinal degeneration and neurological dysfunction. *Hum. Mol. Genet.*, **24**, 3908–3917.
74. Rual, J.F., Hirozane-Kishikawa, T., Hao, T., Bertin, N., Li, S., Dricot, A., Li, N., Rosenberg, J., Lamesch, P., Vidalain, P.O. *et al.* (2004) Human ORFeome version 1.1: a platform for reverse proteomics. *Genome Res.*, **14**, 2128–2135.
75. Lamesch, P., Li, N., Milstein, S., Fan, C., Hao, T., Szabo, G., Hu, Z., Venkatesan, K., Bethel, G., Martin, P. *et al.* (2007) hORFeome v3.1: a resource of human open reading frames representing over 10,000 human genes. *Genomics*, **89**, 307–315.
76. Wang, X.J., Cao, Q., Liu, X., Wang, K.T., Mi, W., Zhang, Y., Li, L. F., LeBlanc, A.C. and Su, X.D. (2010) Crystal structures of human caspase 6 reveal a new mechanism for intramolecular cleavage self-activation. *EMBO Rep.*, **11**, 841–847.
77. Thomas, P.D., Campbell, M.J., Kejariwal, A., Mi, H., Karlak, B., Daverman, R., Diemer, K., Muruganujan, A. and Narechania, A. (2003) PANTHER: a library of protein families and subfamilies indexed by function. *Genome Res.*, **13**, 2129–2141.
78. Verspurten, J., Gevaert, K., Declercq, W. and Vandenabeele, P. (2009) SitePredicting the cleavage of proteinase substrates. *Trends Biochem. Sci.*, **34**, 319–323.
79. Hamosh, A., Scott, A.F., Amberger, J.S., Bocchini, C.A. and McKusick, V.A. (2005) Online Mendelian Inheritance in

Man (OMIM), a knowledgebase of human genes and genetic disorders. *Nucleic Acids Res.*, **33**, D514–D517.
80. Barrios-Rodiles, M., Brown, K.R., Ozdamar, B., Bose, R., Liu, Z., Donovan, R.S., Shinjo, F., Liu, Y., Dembowy, J., Taylor, I. W. *et al.* (2005) High-throughput mapping of a dynamic signaling network in mammalian cells. *Science*, **307**, 1621–1625.
81. Braun, P., Tasan, M., Dreze, M., Barrios-Rodiles, M., Lemmens, I., Yu, H., Sahalie, J.M., Murray, R.R., Roncari, L., de Smet, A.S. *et al.* (2009) An experimentally derived confidence score for binary protein–protein interactions. *Nat. Methods*, **6**, 91–97.
82. Hermel, E., Gafni, J., Propp, S.S., Leavitt, B.R., Wellington, C.L., Young, J.E., Hackam, A.S., Logvinova, A.V., Peel, A.L., Chen, S. F. *et al.* (2004) Specific caspase interactions and amplification are involved in selective neuronal vulnerability in Huntington's disease. *Cell Death Differ.*, **11**, 424–438.
83. Suter, B., Fontaine, J.F., Yildirimman, R., Rasko, T., Schaefer, M.H., Rasche, A., Porras, P., Vazquez-Alvarez, B.M., Russ, J., Rau, K. *et al.* (2013) Development and application of a DNA microarray-based yeast two-hybrid system. *Nucleic Acids Res.*, **41**, 1496–1507.
84. Hodges, A., Strand, A.D., Aragaki, A.K., Kuhn, A., Sengstag, T., Hughes, G., Elliston, L.A., Hartog, C., Goldstein, D.R., Thu, D. *et al.* (2006) Regional and cellular gene expression changes in human Huntington's disease brain. *Hum. Mol. Genet.*, **15**, 965–977.
85. Kuhn, A., Thu, D., Waldvogel, H.J., Faull, R.L. and Luthi-Carter, R. (2011) Population-specific expression analysis (PSEA) reveals molecular changes in diseased brain. *Nat. Methods*, **8**, 945–947.
86. Stroedicke, M., Bounab, Y., Strempel, N., Klockmeier, K., Yigit, S., Friedrich, R.P., Chaurasia, G., Li, S., Hesse, F., Riechers, S.P. *et al.* (2015) Systematic interaction network filtering identifies CRMP1 as a novel suppressor of huntingtin misfolding and neurotoxicity. *Genome Res.*, **25**, 701–713.
87. Liu, Y., Conaway, L., Rutherford Bethard, J., Al-Ayoubi, A.M., Thompson Bradley, A., Zheng, H., Weed, S.A. and Eblen, S.T. (2013) Phosphorylation of the alternative mRNA splicing factor 45 (SPF45) by Clk1 regulates its splice site utilization, cell migration and invasion. *Nucleic Acids Res.*, **41**, 4949–4962.
88. Lee, K.K., Murakawa, M., Nishida, E., Tsubuki, S., Kawashima, S., Sakamaki, K. and Yonehara, S. (1998) Proteolytic activation of MST/Krs, STE20-related protein kinase, by caspase during apoptosis. *Oncogene*, **16**, 3029–3037.
89. Deng, Y., Pang, A. and Wang, J.H. (2003) Regulation of mammalian STE20-like kinase 2 (MST2) by protein phosphorylation/dephosphorylation and proteolysis. *J. Biol. Chem.*, **278**, 11760–11767.
90. Lee, K.K., Ohyama, T., Yajima, N., Tsubuki, S. and Yonehara, S. (2001) MST, a physiological caspase substrate, highly sensitizes apoptosis both upstream and downstream of caspase activation. *J. Biol. Chem.*, **276**, 19276–19285.
91. Kim, D., Shu, S., Coppola, M.D., Kaneko, S., Yuan, Z.Q. and Cheng, J.Q. (2010) Regulation of proapoptotic mammalian ste20-like kinase MST2 by the IGF1-Akt pathway. *PLoS ONE*, **5**, e9616.
92. Bowles, K.R. and Jones, L. (2014) Kinase signalling in Huntington's disease. *J. Huntington's Dis.*, **3**, 89–123.
93. Ooi, J., Hayden, M.R. and Pouladi, M.A. (2014) Inhibition of excessive monoamine oxidase A/B activity protects against stress-induced neuronal death in Huntington disease. *Mol. Neurobiol.*, in press.
94. Janicke, R.U., Sprengart, M.L., Wati, M.R. and Porter, A.G. (1998) Caspase-3 is required for DNA fragmentation and morphological changes associated with apoptosis. *J. Biol. Chem.*, **273**, 9357–9360.
95. Pompl, P.N., Yemul, S., Xiang, Z., Ho, L., Haroutunian, V., Purohit, D., Mohs, R. and Pasinetti, G.M. (2003) Caspase gene expression in the brain as a function of the clinical progression of Alzheimer disease. *Arch. Neurol.*, **60**, 369–376.
96. Gervais, F.G., Xu, D., Robertson, G.S., Vaillancourt, J.P., Zhu, Y., Huang, J., LeBlanc, A., Smith, D., Rigby, M., Shearman, M.S. *et al.* (1999) Involvement of caspases in proteolytic cleavage of Alzheimer's amyloid-beta precursor protein and amyloidogenic A beta peptide formation. *Cell*, **97**, 395–406.
97. Lu, D.C., Rabizadeh, S., Chandra, S., Shayya, R.F., Ellerby, L. M., Ye, X., Salvesen, G.S., Koo, E.H. and Bredesen, D.E. (2000) A second cytotoxic proteolytic peptide derived from amyloid beta-protein precursor. *Nat. Med.*, **6**, 397–404.
98. Klaiman, G., Petzke, T.L., Hammond, J. and LeBlanc, A.C. (2008) Targets of caspase-6 activity in human neurons and Alzheimer disease. *Mol. Cell Proteomics*, **7**, 1541–1555.
99. Ju, W., Valencia, C.A., Pang, H., Ke, Y., Gao, W., Dong, B. and Liu, R. (2007) Proteome-wide identification of family member-specific natural substrate repertoire of caspases. *Proc. Natl Acad. Sci. USA*, **104**, 14294–14299.
100. Jung, J.Y., Lee, S.R., Kim, S., Chi, S.W., Bae, K.H., Park, B.C., Kim, J.H. and Park, S.G. (2014) Identification of novel binding partners for caspase-6 using a proteomic approach. *J. Microbiol. Biotechnol.*, **24**, 714–718.
101. Ghavidel, A., Cagney, G. and Emili, A. (2005) A skeleton of the human protein interactome. *Cell*, **122**, 830–832.
102. von Mering, C., Krause, R., Snel, B., Cornell, M., Oliver, S.G., Fields, S. and Bork, P. (2002) Comparative assessment of large-scale data sets of protein–protein interactions. *Nature*, **417**, 399–403.
103. Waldron-Roby, E., Ratovitski, T., Wang, X., Jiang, M., Watkin, E., Arbez, N., Graham, R.K., Hayden, M.R., Hou, Z., Mori, S. *et al.* (2012) Transgenic mouse model expressing the caspase 6 fragment of mutant huntingtin. *J. Neurosci.*, **32**, 183–193.
104. Zhao, M., Su, J., Head, E. and Cotman, C.W. (2003) Accumulation of caspase cleaved amyloid precursor protein represents an early neurodegenerative event in aging and in Alzheimer's disease. *Neurobiol. Dis.*, **14**, 391–403.
105. Guo, H., Albrecht, S., Bourdeau, M., Petzke, T., Bergeron, C. and LeBlanc, A.C. (2004) Active caspase-6 and caspase-6-cleaved tau in neuropil threads, neuritic plaques, and neurofibrillary tangles of Alzheimer's disease. *Am. J. Pathol.*, **165**, 523–531.
106. Rohn, T.T., Head, E., Nesse, W.H., Cotman, C.W. and Cribbs, D.H. (2001) Activation of caspase-8 in the Alzheimer's disease brain. *Neurobiol. Dis.*, **8**, 1006–1016.
107. Ramcharitar, J., Albrecht, S., Afonso, V.M., Kaushal, V., Bennett, D.A. and Leblanc, A.C. (2013) Cerebrospinal fluid tau cleaved by caspase-6 reflects brain levels and cognition in aging and Alzheimer disease. *J. Neuropathol. Exp. Neurol.*, **72**, 824–832.
108. Harris, J.A., Devidze, N., Halabisky, B., Lo, I., Thwin, M.T., Yu, G.Q., Bredesen, D.E., Masliah, E. and Mucke, L. (2010) Many neuronal and behavioral impairments in transgenic mouse models of Alzheimer's disease are independent of caspase cleavage of the amyloid precursor protein. *J. Neurosci.*, **30**, 372–381.
109. Zhang, Y., Leavitt, B.R., Van Raamsdonk, J.M., Dragatsis, I., Goldowitz, D., MacDonald, M.E., Hayden, M.R. and Friedlander, R.M. (2006) Huntingtin inhibits caspase-3 activation. *EMBO J.*, **25**, 5896–5906.

110. Rigamonti, D., Sipione, S., Goffredo, D., Zuccato, C., Fossale, E. and Cattaneo, E. (2001) Huntingtin's neuroprotective activity occurs via inhibition of procaspase-9 processing. *J. Biol. Chem.*, **276**, 14545–14548.
111. La Spada, A.R. and Morrison, R.S. (2005) The power of the dark side: Huntington's disease protein and p53 form a deadly alliance. *Neuron*, **47**, 1–3.
112. Tourette, C., Li, B., Bell, R., O'Hare, S., Kaltenbach, L.S., Mooney, S.D. and Hughes, R.E. (2014) A large scale Huntingtin protein interaction network implicates Rho GTPase signaling pathways in Huntington disease. *J. Biol. Chem.*, **289**, 6709–6726.
113. Xifro, X., Anglada-Huguet, M., Rue, L., Saavedra, A., Perez-Navarro, E. and Alberch, J. (2011) Increased 90-kDa ribosomal S6 kinase (Rsk) activity is protective against mutant huntingtin toxicity. *Mol. Neurodegener.*, **6**, 74.
114. Plotkin, J.L., Day, M., Peterson, J.D., Xie, Z., Kress, G.J., Rafalovich, I., Kondapalli, J., Gertler, T.S., Flajolet, M., Greengard, P. *et al.* (2014) Impaired TrkB receptor signaling underlies corticostriatal dysfunction in Huntington's disease. *Neuron*, **83**, 178–188.
115. Gines, S., Ivanova, E., Seong, I.S., Saura, C.A. and MacDonald, M.E. (2003) Enhanced Akt signaling is an early pro-survival response that reflects N-methyl-D-aspartate receptor activation in Huntington's disease knock-in striatal cells. *J. Biol. Chem.*, **278**, 50514–50522.
116. Ehrnhoefer, D.E., Skotte, N.H., Ladha, S., Nguyen, Y.T., Qiu, X., Deng, Y., Huynh, K.T., Engemann, S., Nielsen, S.M., Becanovic, K. *et al.* (2014) p53 increases caspase-6 expression and activation in muscle tissue expressing mutant huntingtin. *Hum. Mol. Genet.*, **23**, 717–729.
117. MacLachlan, T.K. and El-Deiry, W.S. (2002) Apoptotic threshold is lowered by p53 transactivation of caspase-6. *Proc. Natl Acad. Sci. USA*, **99**, 9492–9497.
118. Checler, F. and Alves da Costa, C. (2014) p53 in neurodegenerative diseases and brain cancers. *Pharmacol. Ther.*, **142**, 99–113.
119. Rosner, M., Hanneder, M., Siegel, N., Valli, A., Fuchs, C. and Hengstschlager, M. (2008) The mTOR pathway and its role in human genetic diseases. *Mutat. Res.*, **659**, 284–292.
120. Niu, Y.L., Li, C. and Zhang, G.Y. (2011) Blocking Daxx trafficking attenuates neuronal cell death following ischemia/reperfusion in rat hippocampus CA1 region. *Arch. Biochem. Biophys.*, **515**, 89–98.
121. Song, J.J. and Lee, Y.J. (2004) Daxx deletion mutant (amino acids 501-625)-induced apoptosis occurs through the JNK/p38-Bax-dependent mitochondrial pathway. *J. Cell. Biochem.*, **92**, 1257–1270.
122. Bojunga, J., Nowak, D., Mitrou, P.S., Hoelzer, D., Zeuzem, S. and Chow, K.U. (2004) Antioxidative treatment prevents activation of death-receptor- and mitochondrion-dependent apoptosis in the hearts of diabetic rats. *Diabetologia*, **47**, 2072–2080.
123. Roubille, F., Combes, S., Leal-Sanchez, J., Barrere, C., Cransac, F., Sportouch-Dukhan, C., Gahide, G., Serre, I., Kupfer, E., Richard, S. *et al.* (2007) Myocardial expression of a dominant-negative form of Daxx decreases infarct size and attenuates apoptosis in an *in vivo* mouse model of ischemia/reperfusion injury. *Circulation*, **116**, 2709–2717.
124. Lukiw, W.J. (2004) Gene expression profiling in fetal, aged, and Alzheimer hippocampus: a continuum of stress-related signaling. *Neurochem. Res.*, **29**, 1287–1297.
125. Colangelo, V., Schurr, J., Ball, M.J., Pelaez, R.P., Bazan, N.G. and Lukiw, W.J. (2002) Gene expression profiling of 12633 genes in Alzheimer hippocampal CA1: transcription and neurotrophic factor down-regulation and up-regulation of apoptotic and pro-inflammatory signaling. *J. Neurosci. Res.*, **70**, 462–473.
126. Akterin, S., Cowburn, R.F., Miranda-Vizuete, A., Jimenez, A., Bogdanovic, N., Winblad, B. and Cedazo-Minguez, A. (2006) Involvement of glutaredoxin-1 and thioredoxin-1 in beta-amyloid toxicity and Alzheimer's disease. *Cell Death Differ.*, **13**, 1454–1465.
127. Corsini, L., Bonnal, S., Basquin, J., Hothorn, M., Scheffzek, K., Valcarcel, J. and Sattler, M. (2007) U2AF-homology motif interactions are required for alternative splicing regulation by SPF45. *Nat. Struct. Mol. Biol.*, **14**, 620–629.
128. Akhavantabasi, S., Akman, H.B., Sapmaz, A., Keller, J., Petty, E.M. and Erson, A.E. (2010) USP32 is an active, membrane-bound ubiquitin protease overexpressed in breast cancers. *Mamm. Genome*, **21**, 388–397.
129. Graves, J.D., Draves, K.E., Gotoh, Y., Krebs, E.G. and Clark, E.A. (2001) Both phosphorylation and caspase-mediated cleavage contribute to regulation of the Ste20-like protein kinase Mst1 during CD95/Fas-induced apoptosis. *J. Biol. Chem.*, **276**, 14909–14915.
130. Graves, J.D., Gotoh, Y., Draves, K.E., Ambrose, D., Han, D.K., Wright, M., Chernoff, J., Clark, E.A. and Krebs, E.G. (1998) Caspase-mediated activation and induction of apoptosis by the mammalian Ste20-like kinase Mst1. *EMBO J.*, **17**, 2224–2234.
131. Lee, K.K. and Yonehara, S. (2002) Phosphorylation and dimerization regulate nucleocytoplasmic shuttling of mammalian STE20-like kinase (MST). *J. Biol. Chem.*, **277**, 12351–12358.
132. van Raam, B.J., Ehrnhoefer, D.E., Hayden, M.R. and Salvesen, G.S. (2013) Intrinsic cleavage of receptor-interacting protein kinase-1 by caspase-6. *Cell Death Differ.*, **20**, 86–96.
133. Suzuki, A., Kusakai, G., Kishimoto, A., Shimojo, Y., Miyamoto, S., Ogura, T., Ochiai, A. and Esumi, H. (2004) Regulation of caspase-6 and FLIP by the AMPK family member ARK5. *Oncogene*, **23**, 7067–7075.
134. Kurokawa, M. and Kornbluth, S. (2009) Caspases and kinases in a death grip. *Cell*, **138**, 838–854.
135. Medina, E.A., Afsari, R.R., Ravid, T., Castillo, S.S., Erickson, K.L. and Goldkorn, T. (2005) Tumor necrosis factor-{alpha} decreases Akt protein levels in 3T3-L1 adipocytes via the caspase-dependent ubiquitination of Akt. *Endocrinology*, **146**, 2726–2735.
136. Warby, S.C., Chan, E.Y., Metzler, M., Gan, L., Singaraja, R.R., Crocker, S.F., Robertson, H.A. and Hayden, M.R. (2005) Huntingtin phosphorylation on serine 421 is significantly reduced in the striatum and by polyglutamine expansion *in vivo*. *Hum. Mol. Genet.*, **14**, 1569–1577.
137. Lee, H.K., Kumar, P., Fu, Q., Rosen, K.M. and Querfurth, H.W. (2009) The insulin/Akt signaling pathway is targeted by intracellular beta-amyloid. *Mol. Biol. Cell*, **20**, 1533–1544.
138. Pouladi, M.A., Xie, Y., Skotte, N.H., Ehrnhoefer, D.E., Graham, R.K., Kim, J.E., Bissada, N., Yang, X.W., Paganetti, P., Friedlander, R.M. *et al.* (2010) Full-length huntingtin levels modulate body weight by influencing insulin-like growth factor 1 expression. *Hum. Mol. Genet.*, **19**, 1528–1538.
139. Stelzl, U., Worm, U., Lalowski, M., Haenig, C., Brembeck, F.H., Goehler, H., Stroedicke, M., Zenkner, M., Schoenherr, A., Koeppen, S. *et al.* (2005) A human protein–protein interaction network: a resource for annotating the proteome. *Cell*, **122**, 957–968.
140. Palidwor, G.A., Shcherbinin, S., Huska, M.R., Rasko, T., Stelzl, U., Arumughan, A., Foulle, R., Porras, P., Sanchez-Pulido, L., Wanker, E.E. *et al.* (2009) Detection of alpha-rod protein

repeats using a neural network and application to huntingtin. *PLoS Comput. Biol.*, **5**, e1000304.
141. Goehler, H., Lalowski, M., Stelzl, U., Waelter, S., Stroedicke, M., Worm, U., Droege, A., Lindenberg, K.S., Knoblich, M., Haenig, C. *et al.* (2004) A protein interaction network links GIT1, an enhancer of huntingtin aggregation, to Huntington's disease. *Mol. Cell*, **15**, 853–865.
142. Kaltenbach, L.S., Romero, E., Becklin, R.R., Chettier, R., Bell, R., Phansalkar, A., Strand, A., Torcassi, C., Savage, J., Hurlburt, A. *et al.* (2007) Huntingtin interacting proteins are genetic modifiers of neurodegeneration. *PLoS Genet.*, **3**, e82.
143. Schaefer, M.H., Fontaine, J.F., Vinayagam, A., Porras, P., Wanker, E.E. and Andrade-Navarro, M.A. (2012) HIPPIE: integrating protein interaction networks with experiment based quality scores. *PLoS ONE*, **7**, e31826.
144. Jain, N., Thatte, J., Braciale, T., Ley, K., O'Connell, M. and Lee, J.K. (2003) Local-pooled-error test for identifying differentially expressed genes with a small number of replicated microarrays. *Bioinformatics*, **19**, 1945–1951.
145. Su, A.I., Wiltshire, T., Batalov, S., Lapp, H., Ching, K.A., Block, D., Zhang, J., Soden, R., Hayakawa, M., Kreiman, G. *et al.* (2004) A gene atlas of the mouse and human protein-encoding transcriptomes. *Proc. Natl Acad. Sci. USA*, **101**, 6062–6067.